Published July 29, 2013

Inherited human OX40 deficiency underlying classic Kaposi sarcoma of childhood

Minji Byun,[1] Cindy S. Ma,[2,3] Arzu Akçay,[4] Vincent Pedergnana,[5,6] Umaimainthan Palendira,[2,3] Jinjong Myoung,[7] Danielle T. Avery,[2] Yifang Liu,[8] Avinash Abhyankar,[1] Lazaro Lorenzo,[5,6] Monika Schmidt,[9] Hye Kyung Lim,[1] Olivier Cassar,[10] Melanie Migaud,[5,6] Flore Rozenberg,[11] Nur Canpolat,[12] Gönül Aydoğan,[4] Bernhard Fleckenstein,[9] Jacinta Bustamante,[5,6,13] Capucine Picard,[5,6,13] Antoine Gessain,[10] Emmanuelle Jouanguy,[1,5,6] Ethel Cesarman,[8] Martin Olivier,[15] Philippe Gros,[16] Laurent Abel,[1,5,6] Michael Croft,[17] Stuart G. Tangye,[2,3] and Jean-Laurent Casanova[1,5,6,14]

[1]St. Giles Laboratory of Human Genetics of Infectious Diseases, Rockefeller Branch, The Rockefeller University, New York, NY 10065
[2]Immunology Program, Garvan Institute of Medical Research, Darlinghurst, New South Wales 2010, Australia
[3]St. Vincent's Clinical School, Faculty of Medicine, University of New South Wales, Darlinghurst, New South Wales 2010, Australia
[4]Department of Pediatric Hematology and Oncology, Kanuni Sultan Suleyman Education and Research Hospital, 34303 Istanbul, Turkey
[5]Laboratory of Human Genetics of Infectious Diseases, Necker Medical School, National Institute of Health and Medical Research (INSERM) U980, 75015 Paris, France
[6]Imagine Institute, Paris Descartes University, 75270 Paris, France
[7]Novartis Institutes for Biomedical Research, Emeryville, CA 94608
[8]Department of Pathology and Laboratory Medicine, Weill Cornell Medical College, New York, NY 10065
[9]Institut für Klinische und Molekulare Virologie, Universität Erlangen-Nürnberg, D-91054 Erlangen, Germany
[10]Epidemiology and Physiopathology of Oncogenic Viruses Unit, Institut Pasteur, 75724 Paris, France
[11]EA1833, Paris Descartes University and Virology Service, Cochin Hospital, 75014 Paris, France
[12]Department of Pediatric Nephrology, Cerrahpasa Faculty of Medicine, Istanbul University, 34156 Istanbul, Turkey
[13]Study Center for Primary Immunodeficiencies and [14]Pediatric Hematology–Immunology Unit, Necker Hospital, AP-HP, 75015 Paris, France
[15]Department of Microbiology and Immunology and [16]Department of Biochemistry, McGill University, Montreal, Quebec H3G 1Y6, Canada
[17]La Jolla Institute for Allergy and Immunology, La Jolla, CA 92037

Kaposi sarcoma (KS), a human herpes virus 8 (HHV-8; also called KSHV)–induced endothelial tumor, develops only in a small fraction of individuals infected with HHV-8. We hypothesized that inborn errors of immunity to HHV-8 might underlie the exceedingly rare development of classic KS in childhood. We report here autosomal recessive OX40 deficiency in an otherwise healthy adult with childhood-onset classic KS. OX40 is a costimulatory receptor expressed on activated T cells. Its ligand, OX40L, is expressed on various cell types, including endothelial cells. We found OX40L was abundantly expressed in KS lesions. The mutant OX40 protein was poorly expressed on the cell surface and failed to bind OX40L, resulting in complete functional OX40 deficiency. The patient had a low proportion of effector memory CD4$^+$ T cells in the peripheral blood, consistent with impaired CD4$^+$ T cell responses to recall antigens in vitro. The proportion of effector memory CD8$^+$ T cells was less diminished. The proportion of circulating memory B cells was low, but the antibody response in vivo was intact, including the response to a vaccine boost. Together, these findings suggest that human OX40 is necessary for robust CD4$^+$ T cell memory and confers apparently selective protective immunity against HHV-8 infection in endothelial cells.

CORRESPONDENCE
Minji Byun:
miby769@rockefeller.edu
OR
min.byun@gmail.com

Abbreviations used: BCG, Bacille Calmette-Guérin; IRES, internal ribosomal entry site; KS, Kaposi sarcoma; PPD, purified protein derivative; SNP, single nucleotide polymorphism; TT, tetanus toxoid; UPR, unfolded protein response; VL, visceral leishmaniasis; VZV, varicella zoster virus; WAS, Wiskott–Aldrich syndrome.

Kaposi sarcoma (KS) is an inflammatory neoplasm affecting cells of endothelial origin (Ganem, 2010) first described by Moritz Kaposi (Kaposi, 1872). The causal infectious agent of all known

© 2013 Byun et al. This article is distributed under the terms of an Attribution–Noncommercial–Share Alike–No Mirror Sites license for the first six months after the publication date (see http://www.rupress.org/terms). After six months it is available under a Creative Commons License (Attribution–Noncommercial–Share Alike 3.0 Unported license, as described at http://creativecommons.org/licenses/by-nc-sa/3.0/).

The Rockefeller University Press $30.00
J. Exp. Med. 2013 Vol. 210 No. 9 1743-1759
www.jem.org/cgi/doi/10.1084/jem.20130592

Supplemental Material can be found at:
/content/suppl/2013/07/25/jem.20130592.DC1.html

The Journal of Experimental Medicine

Downloaded from on November 4, 2016

Published July 29, 2013

forms of KS is human herpes virus 8 (HHV-8), also known as KS-associated herpes virus (KSHV; Chang et al., 1994). More than 100 million people are infected with HHV-8, with a heterogeneous worldwide distribution (Plancoulaine et al., 2002). Infection with HHV-8 is asymptomatic in the vast majority of cases (Wang et al., 2001; Andreoni et al., 2002). Only a very small proportion of HHV-8–infected individuals develop KS in their lifetime (Davidovici et al., 2001). Acquired immunodeficiency is a strong KS-predisposing factor; HIV coinfection (epidemic KS) and transplantation-related immunosuppression (iatrogenic KS) increase the risk of KS by factors of at least 3,000 and 100, respectively (Jensen et al., 1999; Serraino et al., 2005; Shiels et al., 2011). Idiopathic cases of KS, striking otherwise healthy individuals with no overt immunological deficit, are mostly reported in the Mediterranean Basin (classic KS) and sub-Saharan Africa (endemic KS). Classic KS is typically an indolent disease of the skin occurring predominantly in the elderly (median age of onset: 65 yr; Iscovich et al., 2000). Classic KS is exceedingly rare in children, with fewer than 40 cases reported since 1960 (Dutz and Stout, 1960; Bisceglia et al., 1988; Akman et al., 1989; Zurrida et al., 1994; Landau et al., 2001; Ferrari et al., 2002; Hussein, 2008; Sahin et al., 2010; Salem et al., 2011; Cakir et al., 2013). The data available before the HIV epidemic suggest that endemic KS is usually more aggressive than the classic form, affecting a younger population (median age of onset: 40 yr), with frequent lymph node involvement (Boshoff and Weiss, 2001). Endemic KS in childhood was rare in Africa in the years before the HIV epidemic, although not as rare as the classic form (Taylor et al., 1972). The rarity of childhood KS contrasts with the relatively high seroprevalence of HHV-8 infection in children <15 yr of age in the Mediterranean region and in Sub-Saharan Africa (Mayama et al., 1998; Andreoni et al., 1999; Gessain et al., 1999). Furthermore, childhood KS, whether it is classic or endemic, runs a more aggressive and disseminated course in children than in adults (Dutz and Stout, 1960; Olweny et al., 1976). Thus, inherited or acquired host factors may underlie classic and endemic KS of childhood.

Inherited immunodeficiencies have been described in two unrelated children with classic KS and other, concurrent, infectious phenotypes: autosomal recessive complete IFN-γ receptor-1 (IFN-γR1) deficiency in a Turkish child with KS and mycobacterial disease (Camcioglu et al., 2004) and X-linked recessive Wiskott–Aldrich syndrome (WAS) in a Tunisian child with KS and EBV lymphoma (Picard et al., 2006). The observation that some children with isolated, classic KS were born to consanguineous parents further suggested that single-gene inborn errors of immunity might underlie such cases (Sahin et al., 2010), as seen in children with other isolated life-threatening infectious diseases (Casanova and Abel, 2007; Alcaïs et al., 2010). Accordingly, autosomal recessive complete STIM1 deficiency was found in a Turkish child with fatal, isolated KS (Byun et al., 2010). Collectively, these findings provided evidence that classic KS in childhood, whether isolated or associated with other infections, may result from single-gene inborn errors of immunity to HHV-8. The three known KS-predisposing genes, *IFNGR1*, *WAS*, and *STIM1*, are pleiotropic and expressed in various cell types, including leukocytes and nonhematopoietic cells. It thus remains unknown which specific cell types and molecular pathways are critical for the effective control of HHV-8 infection. We therefore searched for new genetic etiologies of classic KS in childhood. We report here the discovery and characterization of autosomal recessive complete OX40 deficiency in a young adult with childhood-onset classic KS, suggesting a nonredundant role of OX40 in T cell–mediated defense against HHV-8.

RESULTS

Homozygous *TNFRSF4* (OX40) mutation in a patient with childhood-onset classic KS

We investigated a 19-yr-old Turkish woman diagnosed with classic KS at the age of 14 yr (II.1 in Fig. 1 A). She had a history of curable visceral leishmaniasis (VL) at the age of 9 yr but remained otherwise healthy. The detailed clinical case report for this patient has been published elsewhere (case 3 in Sahin et al. [2010]). The consanguinity of her parents (I.1 and I.2), who are HHV-8 seropositive but KS free, suggested that susceptibility to KS in this patient followed an autosomal recessive mode of inheritance. For the identification of chromosomal intervals linked to KS, we performed genome-wide linkage analysis by homozygosity mapping. Genotype information of a healthy sibling (II.3) with positive HHV-8 serology was also included in the linkage analysis. In total, we identified 37 regions with positive LOD (logarithm of the odds) scores, with a combined size of 96 Mb (Table S1). We also performed whole-exome sequencing with the patient's genomic DNA. Whole-exome sequencing identified 32,471 variants, most of which were present in public databases (NCBI dbSNP Build 135, 1000 Genomes release 13, and Exome Variant Server data release ESP6500SI) or our own database (>600 whole-exome sequences from patients with conditions other than KS). Of the 520 variants unique to the patient, 25 were homozygous, 5 of which were within the linked intervals (Table S2). Two resulted in amino acid sequence changes: a missense variant of *OXA1L* and a missense variant of *TNFRSF4*. The *OXA1L* variant was considered unlikely to be damaging because the affected residue was not evolutionarily conserved and the missense variation was predicted to be benign by both PolyPhen-2 (Adzhubei et al., 2010) and SIFT (Kumar et al., 2009). In addition, its surrounding region was homozygous in another healthy sibling (II.2). Although the HHV-8 serology for II.2 was unknown, he had likely been exposed to HHV-8 via close contact with the other family members (Plancoulaine et al., 2000). In contrast, the *TNFRSF4* variant was heterozygous in II.2 (Fig. 1 A). This variant was a strong candidate because *TNFRSF4* encodes OX40 (CD134), a co-stimulatory molecule which has been implicated in long-term T cell immunity (Croft, 2010). OX40 belongs to the TNF receptor (TNFR) superfamily, a group of type I membrane proteins. The missense variant p.

Downloaded from on November 4, 2016

Published July 29, 2013

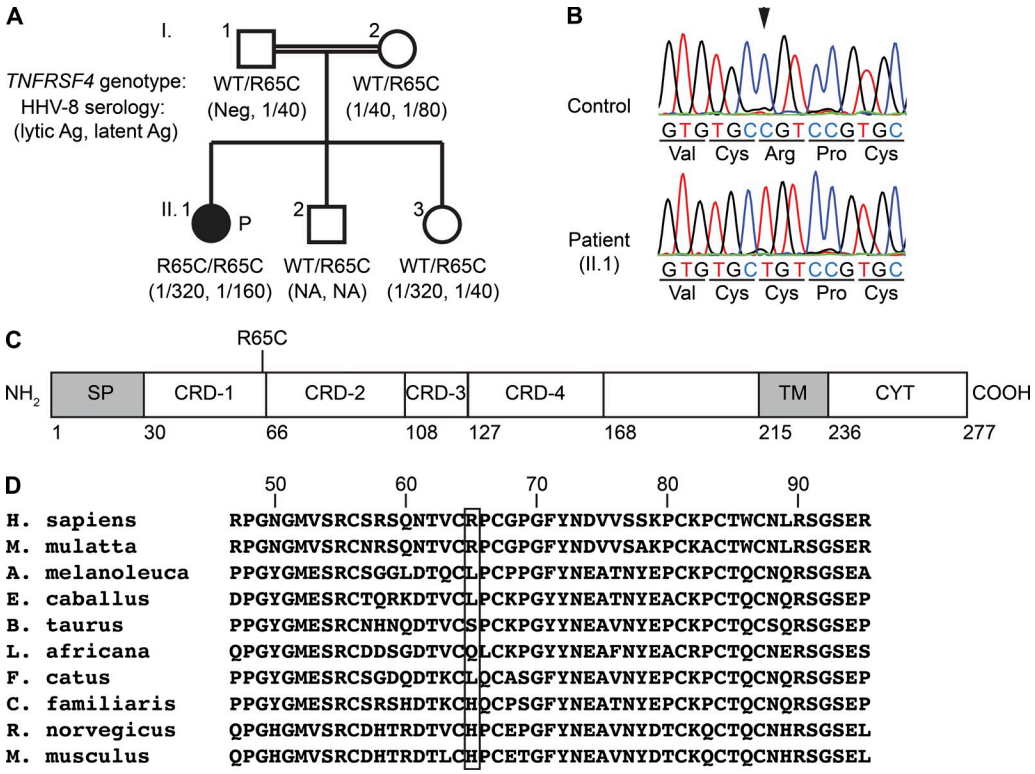


Figure 1. Homozygous *TNFRSF4* mutation in a patient with classic KS. (A) Family pedigree with *TNFRSF4* allele segregation. The black-filled symbol indicates the patient (P). Anti-HHV-8 antibody titers, assessed in serum samples collected 3 yr after the initial HHV-8 serology (case 3 in Sahin et al. [2010]), are indicated in parentheses. Ag, antigen; NA, data not available; Neg, negative. (B) Confirmation of the single nucleotide substitution c.193C>T (indicated by an arrowhead) by Sanger sequencing. *TNFRSF4* exon 2 was amplified by PCR from genomic DNA from a healthy control and the patient. Representative chromatograms for three independent experiments are shown. (C) Schematic representation of OX40 protein structure. Numbers shown below the scheme indicate the amino acid residue number. CRD, cysteine-rich domain; CYT, cytosolic domain; SP, signal peptide; TM, transmembrane domain. (D) Multiple sequence alignment of human *TNFRSF4* and its orthologues. The Arg65 residue of human OX40 (top row) and the corresponding residues in the other species are boxed.

Arg65Cys (R65C), resulting from C to T substitution at nucleotide position 193 (c.193C>T), affects the first of four cysteine-rich domains in the extracellular region of OX40 (Fig. 1, B and C). The arginine residue in position 65 has not been conserved throughout evolution (Fig. 1 D). However, it is adjacent to the highly conserved Cys64 residue, which forms a disulfide bond with another highly conserved residue, Cys46 (Compaan and Hymowitz, 2006). Introduction of an additional cysteine residue in position 65 may impair the correct disulfide bond formation. R65C variation was predicted to be damaging by both PolyPhen-2 and SIFT. The homozygous R65C variation was confirmed by Sanger sequencing (Fig. 1 B). Consistent with an autosomal recessive trait, both parents and two siblings of the patient were found to be heterozygous for the R65C variation (Fig. 1 A). Finally, the R65C variation was not found in 185 Turkish controls and 973 individuals from the HGDP-CEPH Human Diversity Panel (Cann et al., 2002), further suggesting that it was not an irrelevant polymorphism.

Low levels of mutant OX40 proteins on the cell surface

OX40 is expressed predominantly on activated T cells in both humans and mice (Croft, 2010). It has been detected on other types of mouse lymphoid cells, including NK and NKT cells, but data concerning its expression on cells other than T cells in humans remain limited. We investigated the impact of the R65C mutation on production of the protein by determining OX40 levels by flow cytometry with a monoclonal antibody, ACT35. No OX40 expression was detectable on unstimulated circulating T cells from both healthy controls and the patient (not depicted). OX40 expression was strongly induced on PHA-activated $CD4^+$ T cells and to a lesser extent on activated $CD8^+$ T cells from healthy controls (Fig. 2, A and B). OX40 levels were lower, but not abolished, on the surface of activated T cells from the patient. This was not caused by a lack of response to PHA because the induction of CD25 expression was normal on the patient's T cells (not depicted). OX40 levels on the surface of PHA-activated T cells from R65C heterozygous family members (I.1, I.2, and II.3) were similar to those of healthy controls (Fig. 2, A and B). The ectopic production of OX40 in Jurkat or HEK-293 cells with retroviral expression vectors containing an internal ribosomal entry site (IRES) followed by GFP resulted in lower levels of R65C mutant protein than of WT protein at the cell surface (Fig. 2 C and not depicted). The lower levels of

Downloaded from on November 4, 2016

Published July 29, 2013

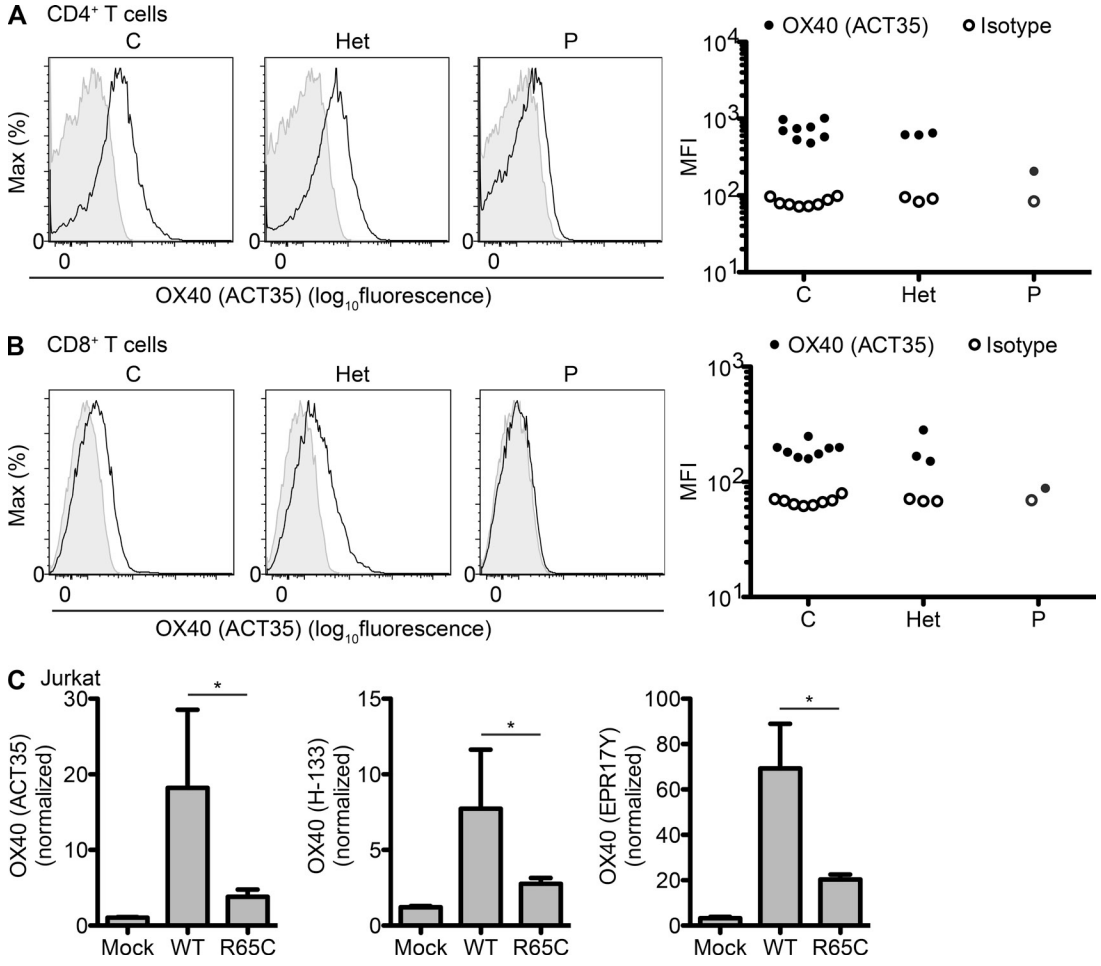


Figure 2. Low levels of mutant OX40 on the cell surface. (A and B) PBMCs from healthy controls (C), R65C heterozygous family members (I.1, I.2, and II.3; Het), and the patient (P) were activated by incubation with PHA for 4 d. Cell surface OX40 levels were determined by flow cytometry with the ACT35 monoclonal antibody. Representative histograms and MFI (mean fluorescence intensity) values for three independent experiments are shown. (A) Gated on the $CD3^+CD4^+$ population ($CD4^+$ T cells). (B) Gated on the $CD3^+CD8^+$ population ($CD8^+$ T cells). (C) Jurkat cells were transduced with bicistronic retroviruses with an empty vector (Mock) or encoding OX40-WT or OX40-R65C, together with IRES-GFP. The MFI of OX40 on GFP^+ cells is shown, as assessed with the antibodies indicated and normalized with respect to isotype controls. The mean values of three independent experiments are plotted. The error bars indicate the SEM. *, $P < 0.05$.

OX40 detected at the cell surface with ACT35 did not result from a change in epitope structure because staining with two other antibodies, H-133 (polyclonal antibody) and EPR17Y (monoclonal antibody), yielded similar results (Fig. 2 C). Overall, these data suggest that the R65C mutation impairs OX40 expression on the cell surface.

Intracellular accumulation of mutant OX40 proteins

We then performed immunoblotting for OX40 proteins. In whole-cell lysates of PHA-activated T cell blasts from healthy controls, most of the OX40 proteins migrated with an approximate mol wt of 50 kD, with a minor fraction observed at 35 kD. The patient's PHA-activated T cell blasts contained a much smaller proportion of the 50-kD form and a much higher proportion of the 35-kD form (Fig. 3 A). Higher levels of the 35-kD form were also observed in R65C heterozygous individuals (I.1, I.2, and II.3). The lower mol wt forms (35 kD) of OX40 were sensitive to endoglycosidase H and resistant to O-glycosidase (Fig. 3 B), indicating they had immature, high-mannose N-linked carbohydrates and no O-linked carbohydrates. Conversely, the higher mol wt forms (50 kD) were endoglycosidase H resistant and O-glycosidase sensitive (Fig. 3 B), indicating they had complex N-linked and O-linked carbohydrates, these modifications being made in the Golgi complex. The biotin labeling of cell surface proteins in HEK-293 cells that expressed OX40 ectopically further demonstrated that the lower mol wt forms were exclusively intracellular (Fig. 3 C). The accumulation of lower mol wt forms of OX40 with immature carbohydrates in the patient's cells thus suggests that most of the newly synthesized mutant OX40 proteins remained in the ER and did not enter the Golgi complex. However, the unfolded protein response (UPR) was not activated in the patient's T cell blasts, as assessed with quantitative RT-PCR to measure the induction of BiP/GRP78

Downloaded from on November 4, 2016

Published July 29, 2013

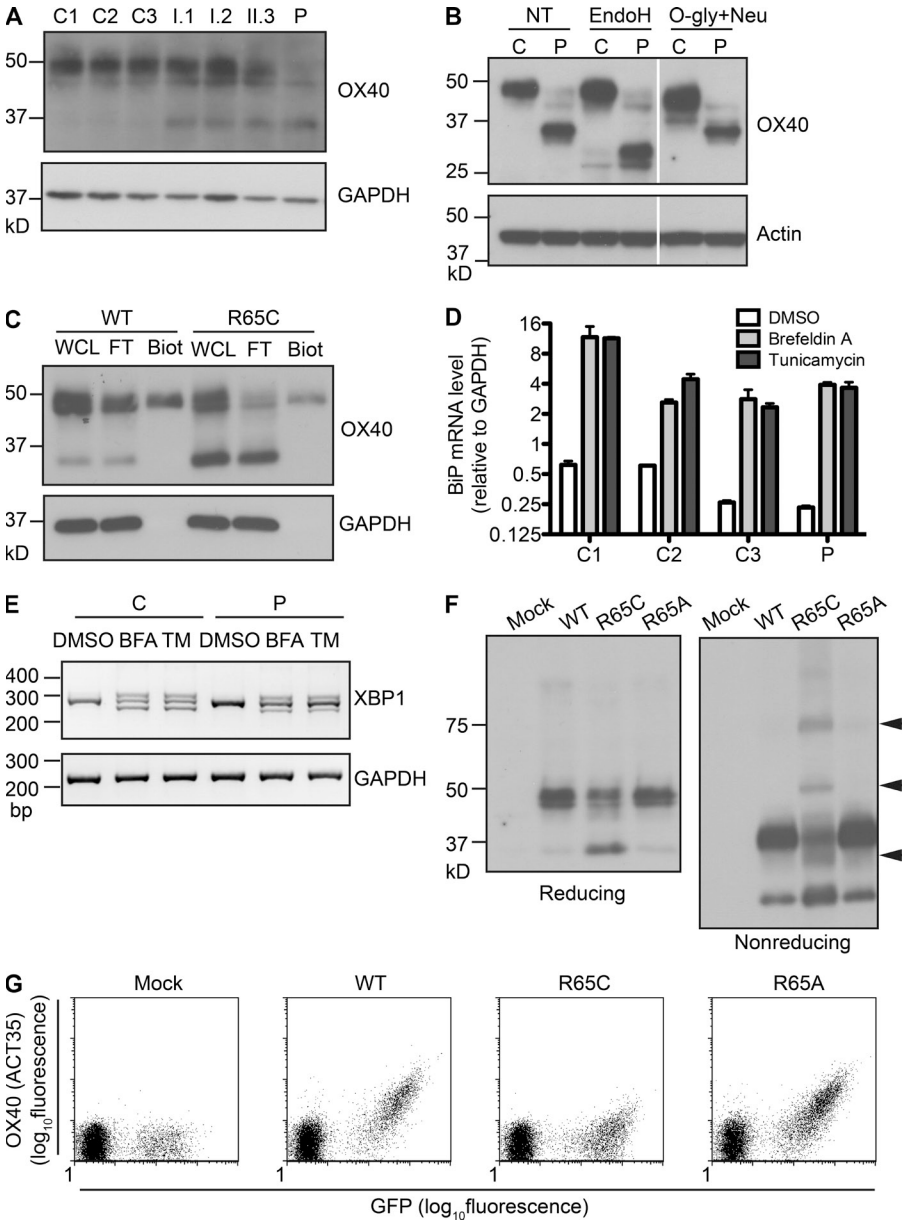


Figure 3. Intracellular accumulation of the mutant OX40 proteins. (A) Immunoblotting of PHA-activated T cell blasts from three healthy controls (C1–C3), R65C heterozygous family members (I.1, I.2, and II.3), and the patient (P) was performed with the anti-OX40 monoclonal antibody EPR17Y. GAPDH served as a loading control. One experiment representative of three performed is shown. (B) Whole-cell lysates of PHA-activated T cell blasts from a healthy control (C) or the patient (P) were treated with the enzymes indicated before immunoblotting. White lines indicate the intervening lanes have been spliced out. One experiment representative of two performed is shown. EndoH, endoglycosidase H; NT, nontreated; O-gly+Neu, O-glycosidase and neuraminidase. (C) HEK-293 cells transduced with retroviral vectors encoding OX40-WT or OX40-R65C were subjected to cell surface biotinylation. Biotinylated proteins were isolated with avidin-coated beads. OX40 immunoblotting was performed on whole-cell lysate (WCL), the flow-through fraction (FT), and the biotinylated fraction (Biot). A GAPDH blot was used to assess whether the biotinylated fraction was free of intracellular proteins. The results of two independent experiments are shown. (D and E) PHA-activated T cell blasts from healthy controls (C1–C3) or the patient (P) were treated with DMSO alone or treated with either Brefeldin A (BFA) or tunicamycin (TM) for 6 h. The results of two independent experiments are shown. (D) The mRNA levels of BiP/GRP78, relative to GAPDH, were assessed by quantitative RT-PCR. Error bars indicate the SEM. (E) PCR was performed using primer pairs that can differentiate various spliced variants of XBP1 mRNA. (F) Whole-cell lysates of HEK-293 cells transduced with retroviral vectors with an empty vector (Mock) or encoding OX40-WT, OX40-R65C, or OX40-R65A were resolved by SDS-PAGE under reducing or nonreducing conditions. The arrowheads indicate protein bands unique to the OX40-R65C sample. One result representative of three independent experiments is shown. (G) Jurkat cells were transduced with bicistronic retroviruses with an empty vector (Mock) or encoding OX40-WT, OX40-R65C, or OX40-R65A, together with IRES-GFP. Cell surface OX40 levels were assessed with ACT35 by flow cytometry. One result representative of three independent experiments is shown.

Downloaded from on November 4, 2016

Published July 29, 2013

mRNA and PCR to detect spliced XBP1 mRNA (Fig. 3, D and E). This was not caused by a general defect in the UPR pathway because Brefeldin A– or tunicamycin-induced activation of the UPR was normal (Fig. 3, D and E). Therefore, the accumulation of mutant OX40 proteins does not seem to induce ER stress.

Introduction of a cysteine at position 65 is deleterious

We hypothesized that the acquisition of an additional cysteine residue in position 65 might interfere with correct disulfide bond formation. Indeed, multiple bands unique to OX40-R65C were observed in nonreducing conditions, probably corresponding to OX40 molecules with abnormal intra- and/or intermolecular disulfide bonds (Fig. 3 F, arrowheads). We investigated the impact of the cysteine residue in position 65 further by generating an OX40-R65A mutant. No accumulation of lower mol wt forms was observed in HEK-293 cells expressing OX40-R65A, and the migration pattern of OX40-R65A proteins in nonreducing conditions was similar to that of OX40-WT proteins (Fig. 3 F). The much lower levels of OX40 expression at the cell surface observed in OX40-R65C–transduced Jurkat and HEK-293 cells were not observed in OX40-R65A–transduced cells (Fig. 3 G and not depicted). These results suggest that the introduction of a cysteine residue at position 65, rather than the loss of the arginine residue normally present, is responsible for the impaired cell surface expression of the OX40-R65C mutant proteins.

R65C is a loss-of-function mutation

We then investigated whether the R65C mutation led to a functional OX40 deficiency. Human OX40 ligand (OX40L), encoded by *TNFSF4*, is a member of the TNF superfamily and a type II membrane protein. Its expression, which is often inducible, has been observed in professional antigen-presenting cells including dendritic cells, macrophages, and B cells, as well as other cell types such as endothelial cells, mast cells, and lymphoid tissue inducer cells (Croft, 2010). Its expression on endothelial cells is of particular interest, as KS is driven by the proliferation of HHV-8–infected endothelial cells (Ganem, 2010). Despite the expression of residual mutant OX40 on the cell surface, binding to soluble recombinant OX40L by PHA-activated T cells of the patient was completely abolished (Fig. 4 A). Lentiviral expression of a cDNA encoding OX40-WT, but not OX40-R65C, rescued OX40L binding in the patient's T cells (Fig. 4 B). Moreover, binding to OX40L was severely impaired in Jurkat cells expressing OX40-R65C, as shown by comparison with cells expressing OX40-WT (16-fold decrease; Fig. 4 C). This defect is much more severe than that in surface expression (three- to fourfold decrease; Fig. 2 C). Similar results were obtained with HEK-293 cells (Fig. 4 C). We assessed the impact of the R65C mutation on T cell co-stimulation in response to membrane-bound OX40L by transducing Vero cells with retroviruses encoding human OX40L or an empty vector. An OX40L-dependent enhancement of cell proliferation was observed in anti-CD3–activated T cells from healthy controls but not in those from the patient (Fig. 4 D). This was not caused by an intrinsic defect in T cell proliferation because the patient's T cells proliferated normally in response to various doses of anti-CD3 antibody alone or PHA (Fig. 4 E). The R65C is thus a loss-of-function allele, and the patient homozygous for this allele displays complete functional OX40 deficiency. These data suggest that two mechanisms underlie the loss of function of the R65C mutant allele: (1) a low level of OX40 proteins on the cell surface and (2) an abolition of the binding to OX40L of the residual OX40 proteins on the cell surface.

Low proportions of nonnaive T cell subsets in the peripheral blood

The total number of leukocytes and the proportions of the major leukocyte subsets in peripheral blood were normal in the patient (Table 1). The proportions of T, B, NK, NKT, and γδ T cells in PBMCs were also similar to those of age-matched healthy controls (Table 1). Given the T cell–specific expression of OX40, we carefully examined various subsets of peripheral blood T cells. The proportions of $CD4^+$ and $CD8^+$ T cells in the lymphocyte gate were normal in the patient (Table 1). The proportion of naive $CD4^+$ T cells was higher in the patient than in healthy controls (Fig. 5 A). This reflected the lower proportions of nonnaive subsets, particularly for the $CD45RA^-CCR7^-$ effector memory (T_{EM}) population, but also for the regulatory T and $CXCR3^+$ (enriched in IFN-γ–producing T cells [Duhen et al., 2012]) subsets (Fig. 5, A and B). The proportions of the $CXCR5^+$ (follicular helper T cells) and $CCR6^+$ (enriched in IL-17–producing T cells) subsets were similar to those of healthy controls. We also examined $CD8^+$ T cell subsets. The proportion of naive $CD8^+$ T cells and that of $CD8^+$ T_{EM} were only higher and lower in the patient than in healthy controls, respectively (Fig. 5 C). We observed no increase in the proportion of the $CD45RA^+CCR7^-$ T_{EMRA} subset, which is often expanded in individuals with chronic viral infection, despite the patient suffering from KS over 5 yr (Fig. 5 C). Peptide–MHC class I multimer staining showed the patient to have low and normal frequencies of circulating CMV- and EBV-specific $CD8^+$ T cells, respectively (Fig. 5 D), with a T_{EM} phenotype (not depicted). We also investigated the levels of various cell surface markers, 2B4, CD127, CD103, CLA, CD57, CX3CR1, CD28, CD62L, CD11a, CD11b, CD27, CD95, granzyme B, and perforin, the expression of which changes during the differentiation of naive $CD4^+$ and $CD8^+$ T cells into memory and effector subsets. No overt difference was noted between the patient and the healthy controls for these markers (not depicted).

Impaired memory $CD4^+$ T cell response to recall antigens

We assessed the function of memory $CD4^+$ T cells in the patient by measuring cytokine production and proliferation in response to a panel of recall antigens in vitro. PBMCs from Bacille Calmette-Guérin (BCG)–vaccinated healthy controls and BCG-vaccinated R65C heterozygous family members secreted large amounts of IFN-γ in response to purified protein derivative (PPD; Fig. 6 A). However, the patient's PBMCs

Downloaded from on November 4, 2016

Published July 29, 2013

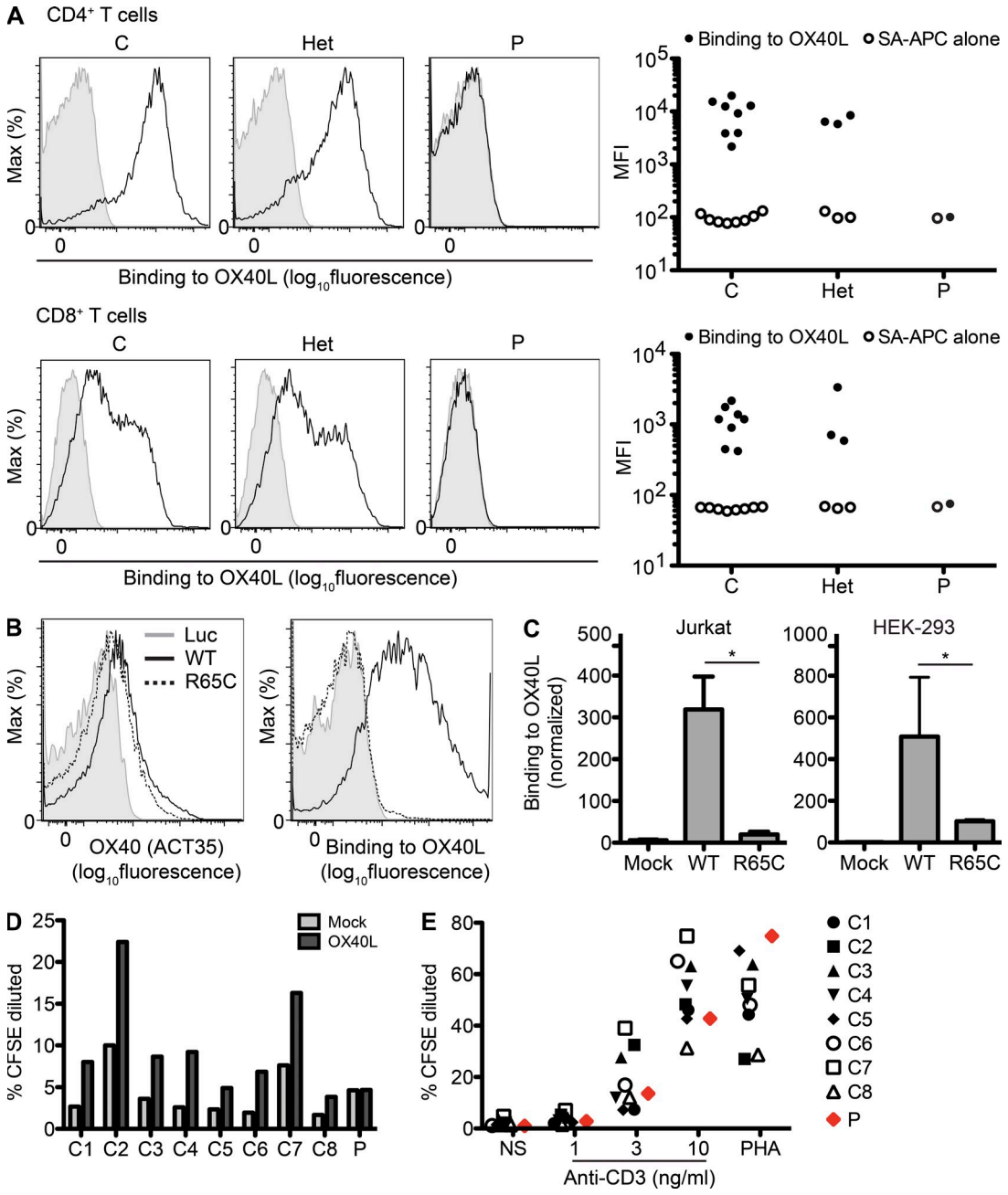


Figure 4. R65C is a loss-of-function mutation. (A) PHA-activated T cell blasts from healthy controls (C), R65C heterozygous family members (Het), or the patient (P) were incubated with biotinylated recombinant soluble OX40L. Unbound OX40L molecules were washed out, and the levels of cell-bound OX40L were measured by flow cytometry with allophycocyanin-labeled streptavidin (SA-APC). Representative histograms and MFIs (mean fluorescence intensities) of $CD3^+CD4^+$ cells ($CD4^+$ T cells) and $CD3^+CD8^+$ cells ($CD8^+$ T cells) in three independent experiments are shown. (B) PHA-activated T cell blasts from the patient were transduced with bicistronic lentiviral vectors encoding luciferase (Luc), OX40-WT, or OX40-R65C, together with IRES-RFP. Cell surface OX40 levels measured with ACT35 and binding to OX40L measured with biotinylated recombinant soluble OX40L are shown for $CD3^+CD4^+RFP^+$ cells. One result representative of two independent experiments is shown. (C) OX40L binding to Jurkat or HEK-293 cells transduced with bicistronic retroviruses with an empty vector (Mock) or encoding OX40-WT or OX40-R65C, together with IRES-GFP, was assessed as in A. The MFIs of OX40L binding for GFP^+ cells, normalized with respect to those for isotype controls, are shown. The mean of three independent experiments is shown. Error bars indicate the SEM. *, $P < 0.05$. (D) CFSE-labeled PBMCs from healthy controls (C1–C8) and the patient (P) were incubated for 3 d with 1 ng/ml of plate-bound anti-CD3 antibody and Vero cells infected with retroviruses either with an empty vector (Vero-Mock) or encoding OX40L (Vero-OX40L). Percentages of CFSE-diluted cells in the $CD3^+CD4^+$ population are plotted. One result representative of two independent experiments is shown. (E) CFSE-labeled PBMCs from healthy controls (C1–C8) and the patient (P) were incubated for 3 d with the indicated concentrations of plate-bound anti-CD3 antibody or PHA. Percentages of CFSE-diluted cells in the $CD3^+CD4^+$ population are plotted. One result representative of two independent experiments is shown.

Downloaded from on November 4, 2016

Published July 29, 2013

Table 1. Counts and proportions of circulating leukocytes

Parameter	Age of the patient at the time of the determination			Normal range
	19.0 yr	19.3 yr	19.6 yr	
Polymorphonuclear neutrophils (/µl)	3,600	4,200	2,400	1,500–3,500
Lymphocytes (/µl)	1,400	1,400	1,320	1,400–3,300
Monocytes (/µl)	500	500	280	210–730
T cells ($CD3^+$) (% lymphocytes)				
Total	71.1	61.4	ND	67.5–77.8
$CD4^+$	38.9	32.2	31.2	26.8–42.7
$CD8^+$	21.3	17.7	18.4	22.1–36.8
B cells ($CD20^+$) (% lymphocyte)	7.1	8.7	ND	8.0–18.3
NK cells ($CD3^-CD56^+$) (% lymphocytes)				
CD56dim	7.9	11.4	ND	3.5–12.3
CD56bright	0.29	0.26	ND	0.03–0.67
NKT cells ($CD3^+V\alpha24^+V\beta11^+$) (% $CD3^+$ cells)	0.17	0.32	ND	0.01–0.30
γδ T cells ($CD3^+V\gamma\delta^+$) (% $CD3^+$ cells)	7.9	15.7	ND	2.4–6.77

Normal range values are from five age-matched healthy controls.

Downloaded from on November 4, 2016

produced only background levels of IFN-γ, similar to those produced by the cells of healthy controls not vaccinated with BCG, despite the patient having been vaccinated twice with BCG (Fig. 6 A). Furthermore, no IFN-γ production by the patient's PBMCs was detectable in response to other recall antigens, including tetanus toxoid (TT) and common viruses (CMV, varicella zoster virus [VZV], HSV-1, and EBV), although positive serological results indicated that the patient had been exposed to these antigens (Fig. 6 B and Table 2). The responses of healthy controls to these recall antigens were variable, but all mounted positive IFN-γ response to at least two of the five non-PPD recall antigens tested (Fig. 6 B). Similar results were obtained for IL-10 (Fig. 6, C and D). Proliferative responses to these antigens, as assessed by CFSE dilution assay, were also weak in the patient's $CD4^+$ T cells (Fig. 6 E). Blocking the OX40–OX40L interaction with neutralizing anti-OX40L antibodies in a similar in vitro recall response assay had no effect on the response of healthy control cells, suggesting that a requirement for OX40–OX40L interactions to elicit in vitro recall responses was not the underlying cause of the defect observed for the patient's cells in this assay (Fig. 6 F). Instead, these results strongly suggest an in vivo deficiency of antigen-specific memory $CD4^+$ T cells in the patient.

Low frequency of circulating memory B cells but intact antibody response in vivo

OX40L can be expressed on activated B cells, and OX40–OX40L interactions may promote T cell–dependent B cell responses in some instances (Morimoto et al., 2000). We thus investigated B cell immunity in the patient. The proportion of $CD10^-CD27^+$ memory B cells within the total B cell population was lower and that of $CD10^-CD27^-$ naive B cells was higher in the patient than in the age-matched healthy controls (Fig. 7 A). This was not caused by a class-switching defect because the proportions of isotype-switched memory B cells (i.e., those expressing IgG and IgA) in the patient were in the normal range (Fig. 7 B). We also studied B cell differentiation in vitro by culturing purified total B cells with CD40L, IL-10, IL-21, and CpG. B cells from the patient gave rise to IgM-secreting plasmablasts with a frequency similar to that observed for healthy controls (Fig. 7 C). In contrast, the frequencies of in vitro–generated total IgG-secreting B cells (Fig. 7 D) as well as the levels of total (Fig. 7 E) and TT-specific (Fig. 7 F) secreted IgG were markedly lower for the patient than the controls. This probably reflects the paucity of memory B cells in the patients' sample, as these cells are responsible for the production of the vast majority of Ig, especially IgG, in in vitro cultures of total B cells (Bryant et al., 2007). Consistent with this defect in memory B cell generation, boosting the patient with TT vaccine had no appreciable effect on the frequency of antigen-specific memory B cells, as measured 4 wk after immunization (Fig. 7 F). However, a boost TT vaccination in the patient substantially increased the serum titer of TT-specific antibody in the patient (Fig. 7 G). Moreover, the serum concentrations of total IgG, IgA, IgM, and IgE and of IgG subclasses (IgG1: 7,270 mg/liter, IgG2: 3,850 mg/liter, IgG3: 866 mg/liter, and IgG4: 192 mg/liter) were within the normal range in the patient, and the titers of various antigen-specific antibodies in the patient's serum were similar to those in healthy family members (Table 2). These data, together with the lack of infectious diseases commonly observed in antibody-deficient patients (Conley et al., 2009), strongly suggest that antibody-mediated immunity is intact in the OX40-deficient patient. These data also suggest that OX40–OX40L interaction is differentially required for the generation of antigen-specific plasma cells versus memory B cells.

OX40L is highly expressed in KS lesions

The 19-yr-old OX40-deficient patient presented no severe infectious or tumoral phenotype other than KS and VL. The

Published July 29, 2013

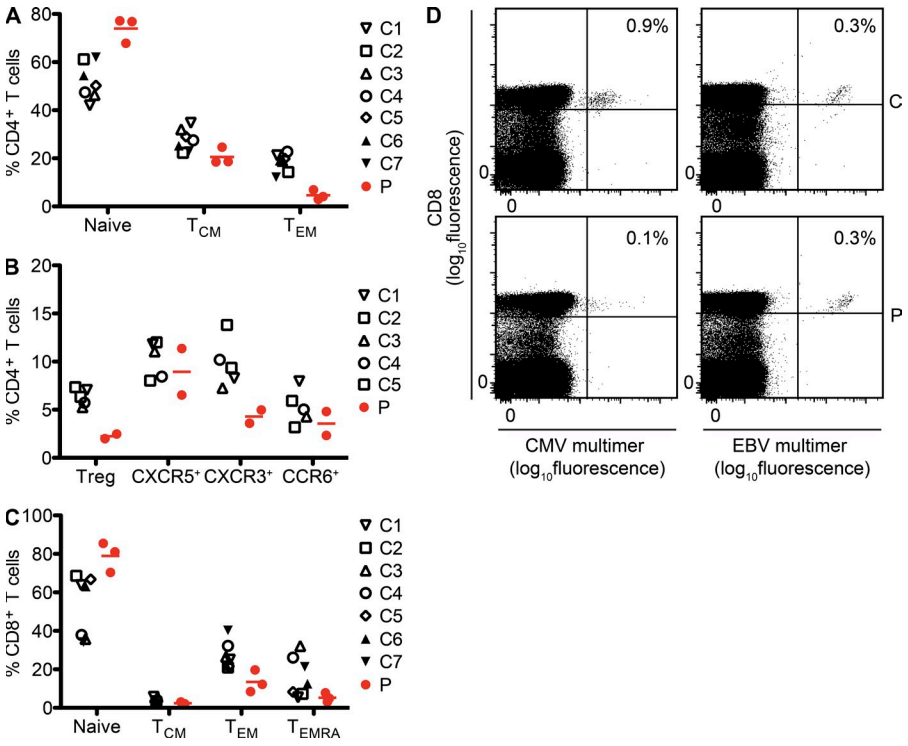


Figure 5. Lower proportions of circulating nonnaive T cell subsets. (A and B) The proportions of the indicated subsets among CD4+ T cells (CD3+CD4+) were assessed in PBMCs collected from five to seven age-matched healthy controls (C) and the patient (P). Two or three independent measurements (of blood drawn at different time points) were performed for the patient (each indicated by a red circle). Mean values are indicated with red horizontal bars. The various subsets were defined as follows: naive ($CD45RA^+CCR7^+$); T_{CM}, T central memory ($CD45RA^-CCR7^+$); T_{EM}, T effector memory ($CD45RA^-CCR7^-$); Treg, T regulatory cells ($CD25^{high}CD127^{low}$); $CXCR5^+$, T follicular helper cells ($CD45RA^-CXCR5^+$); $CXCR3^+$, IFN-γ–producing T cells ($CD45RA^-CXCR5^-CXCR3^+CCR6^-$); and $CCR6^+$, IL-17–producing T cells ($CD45RA^-CXCR5^-CXCR3^-CCR6^+$). (C) Proportions of $CD8^+$ T cell ($CD3^+CD8^+$) subsets, assessed as in A, are shown. The various subsets were defined as follows: naive ($CD45RA^+CCR7^+$); T_{CM} ($CD45RA^-CCR7^+$); T_{EM} ($CD45RA^-CCR7^-$); and T_{EMRA}, $CD45RA^+$ revertant memory T cells ($CD45RA^+CCR7^-$). (D) The frequency of antigen-specific $CD8^+$ T cells ($CD3^+CD8^+$) in an age-matched control (C) or the patient (P) was assessed with HLA-A*0201 multimers loaded with peptides derived from CMV antigen pp65 or EBV antigen BMLF-1.

pathogenesis of KS and VL may involve the systemic $CD4^+$ memory T cell deficiency seen in the patient. The essential and apparently selective role of OX40 in protective immunity to HHV-8, and perhaps to *Leishmania*, may also reflect the tissue tropism of these pathogens. Indeed, the expression of OX40L on endothelial cells has been reported previously both in vitro (Imura et al., 1996; Kunitomi et al., 2000) and in situ (Souza et al., 1999; Papadopoulos et al., 2013). We also documented the expression of OX40L on primary lymphatic and blood endothelial cells (Fig. 8 A). Furthermore, we observed an abundant expression of OX40L with immunohistochemistry in tumor biopsies from AIDS-related KS patients (Fig. 8, B–G). A functional OX40–OX40L interaction between $CD4^+$ T cells and HHV-8–infected endothelial cells, as the antigen-presenting cells, may be required for the generation of protective immunity to HHV-8 in endothelial cells and to prevent the development of KS. Interestingly, we found that the expression of OX40L in LANA (HHV-8 latency-associated nuclear antigen)-positive cells was lower than that of LANA-negative cells lining vascular spaces in the vicinity (Fig. 8, B–E). This may be caused by an HHV-8–induced down-regulation of OX40L to avoid immune surveillance. But the down-regulation may not be complete, and/or T cells may receive OX40L stimulation in trans from the neighboring cells. In any case, we speculate that KS may have occurred in the OX40-deficient patient as a result of the combination of the systemic deficiency in $CD4^+$ memory T cells and the local deficiency of OX40–OX40L interaction between T cells and HHV-8–infected endothelial cells at the disease sites.

DISCUSSION

We describe here autosomal recessive complete OX40 deficiency in a patient with childhood-onset classic KS. Our data strongly support a causal relationship between OX40 deficiency and the development of KS in this patient. The homozygous missense mutation in OX40 is the only nonsynonymous private variation, found by whole-exome sequencing and genome-wide linkage analysis, that segregated with the KS phenotype in this kindred. We further demonstrated that the patient's OX40 allele has a complete loss of function with in-depth biochemical and cellular characterization. The immunological phenotype of the patient largely overlaps with that of OX40-deficient mice (Kopf et al., 1999; Pippig et al., 1999), including, in particular, an impairment of memory

Downloaded from on November 4, 2016

Published July 29, 2013

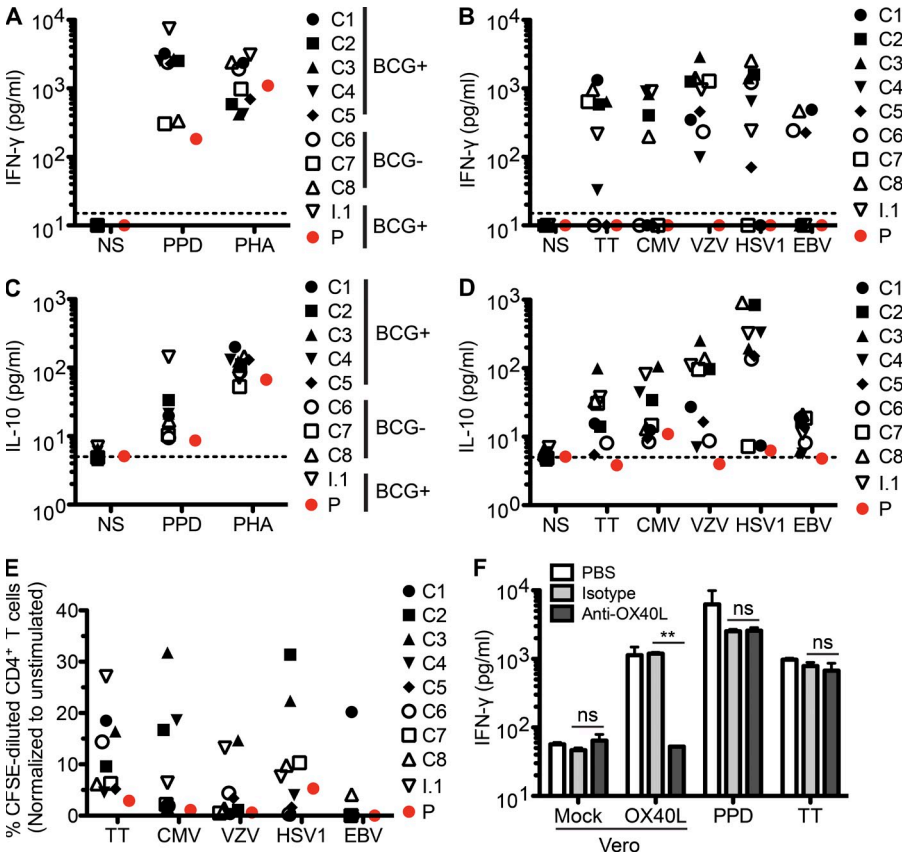


Figure 6. Impaired CD4⁺ T cell recall antigen response. (A and C) PBMCs from eight healthy controls (C1–C8), an R65C heterozygous family member (I.1), and the patient (P) were stimulated with PPD or PHA for 5 d. IFN-γ (A) or IL-10 (C) levels in the supernatant were measured by ELISA. The dotted lines indicate the limit of detection. One result representative of three independent experiments is shown. BCG+, BCG vaccinated; BCG−, no prior BCG vaccination; NS, nonstimulated. (B and D) IFN-γ (B) or IL-10 (D) production in response to various recall antigens was assessed as in A and C. Except for TT, which was provided as purified protein, the recall antigens were provided as virus-infected crude cell lysate. A lysate of uninfected cells tested in the same experiment did not trigger IFN-γ production (not depicted). The dotted lines indicate the limit of detection. One result representative of three independent experiments is shown. (E) CFSE-labeled PBMCs were incubated with the indicated recall antigens for 6 d. T cell proliferation was assessed by determining the proportion of cells with CFSE levels lower than the undivided peak. Results are shown for CD4⁺ T cells (CD3⁺CD4⁺). One result representative of three independent experiments is shown. (F) PBMCs from two healthy controls were incubated with 1 ng/ml of plate-bound anti-CD3 and Vero cells infected with retroviruses with an empty vector (Vero-Mock) or encoding OX40L (Vero-OX40L) for 3 d, or PPD or TT for 6 d. PBS, isotype antibody, or anti-OX40L antibody was added every other day to a concentration of 1 µg/ml. IFN-γ levels in the culture supernatant were measured by ELISA. Means and SEM from two experiments for one of the healthy controls are shown. **, $P < 0.01$; ns, not significant.

CD4⁺ T cell response to recall antigens (Gramaglia et al., 2000; Croft, 2003, 2010). A defect in CD4⁺ T cells has been observed in other patients with genetic susceptibility to KS: the IFN-γR1–deficient patient had CD4⁺ T lymphopenia at the time of KS onset (Camcioglu et al., 2004), the WAS patient presented a severe defect in T cell activation (Picard et al., 2006), and although the immunological phenotype of the STIM1-deficient KS patient could not be assessed (Byun et al., 2010), other individuals with STIM1 deficiency have been shown to display impaired CD4⁺ T cell activation (Fuchs et al., 2012). Furthermore, patients with acquired immunodeficiencies affecting CD4⁺ T cells, such as AIDS patients and transplant recipients treated with calcineurin inhibitors, present an increased risk of developing KS (Lebbé et al., 2008; Shiels et al., 2011). Finally, harboring biallelic loss-of-function OX40 mutations compromising CD4⁺ T cell immunity and developing classic KS in childhood are both exceedingly rare events (each estimated to affect less than one in 10 million individuals [see Materials and methods]). Overall, these data strongly suggest that KS in this patient is a consequence of OX40 deficiency.

Interestingly, the patient had a history of curable VL at 9 yr of age. VL is a parasitic disease caused by *Leishmania donovani* and *L. infantum* (*chagasi*). It is fatal if left untreated (Chappuis et al., 2007). The estimated annual incidence of VL is much higher than that of classic KS in childhood (*L. infantum* alone accounts for ∼50,000 cases worldwide). The causal relationship between OX40 deficiency and VL in this patient is thus less evident, but nonetheless plausible for the following reasons: (a) most *Leishmania*-infected individuals do not develop clinical illness, as demonstrated by the relatively high proportions of asymptomatic carriers in endemic areas (0.6–71.3%,

Downloaded from on November 4, 2016

Published July 29, 2013

Table 2. Ig levels and serological results for common viruses

Parameter	Patient (normal range)	I.1	I.2	II.3
Age (yr)	19	38	36	14
Ig				
IgG (g/liter)	12.6 (6.6–12.8)	ND	ND	ND
IgA (g/liter)	1.2 (0.7–3.44)	ND	ND	ND
IgM (g/liter)	0.8 (0.5–1.09)	ND	ND	ND
IgE (IU/ml)	20 (<100)	ND	ND	ND
Specific antibody				
EBV				
Anti-EBNA IgG (<20)[a] (U/ml)	<3.0	146.0	<3.0	<3.0
Anti-VCA IgG (<20)[a] (U/ml)	55.0	244.0	<10.0	653.0
Anti-VCA IgM (<40)[a] (IU/ml)	22.9	ND	1.7	1.5
Parvovirus B19				
IgG (<1.1)[a]	3.5	7.9	32.5	10.4
IgM (<1.1)[a]	0.1	0.3	0.1	0.1
CMV				
IgG (<14.0)[a] (AU/ml)	82.4	94.8	101.0	100.0
IgM (<22.0)[a] (AU/ml)	<5.0	<5.0	5.46	<5.0
HSV-1 and HSV-2				
IgG (<1.1)[a]	29.7	12.2	>30.0	29.7
VZV				
IgG (<150)[a] (mIU/ml)	764.6	1,315.0	419.3	835.6
Rubella				
IgG (<10)[a] (IU/ml)	135	28	16	35
Mumps				
IgG (<50)[a]	152	120	178	240
Measles				
IgG (<16.5)[a] (AU/ml)	18.0	288.0	>300.0	>300.0

[a]Indicates the threshold for each assay.

depending on the region and the method of detection; Michel et al., 2011); (b) familial clustering and ethnic differences have suggested a role for host genetic factors in determining the outcome ofVL (Cabello et al., 1995; Ibrahim et al., 1999; Khalil et al., 2002; Bucheton et al., 2003); (c) IL-12Rβ1 deficiency was reported as the first genetic etiology of familial VL (Sanal et al., 2007), although susceptibility to VL was a rare finding in IL-12Rβ1–deficient patients (1 out of 141 patients; de Beaucoudrey et al., 2010); (d) the risk of developing clinical VL is higher in patients coinfected with HIV (Murray, 1999; Kumar and Nylén, 2012); (e) *Leishmania* resides in macrophages, which are known to express OX40L; (f) an OX40 agonist has been shown to enhance the killing of amastigotes in C57BL/6 mice infected with *L. donovani* (Zubairi et al., 2004); and (g) we showed that liver *L. infantum* load was much higher in infected OX40-deficient mice than WT mice (unpublished data). The discovery of other genetic disorders underlying VL may further elucidate the mechanisms by which OX40 contributes to protective immunity against *Leishmania*.

The narrow infectious phenotype of the OX40-deficient patient is intriguing. OX40 is probably not essential for immunity to most childhood pathogens, or at least those to which this patient had been exposed. No higher morbidity or viral burden was reported in OX40- or OX40L-deficient mice than in the corresponding control groups after acute infections with influenza virus, murine CMV, or vaccinia virus, despite apparent defects in T cell memory (Hendriks et al., 2005; Humphreys et al., 2007; Salek-Ardakani et al., 2008). However, OX40-deficient mice infected with the clone 13 isolate of LCMV, which establishes persistent infection in mice, failed to clear the virus efficiently (Boettler et al., 2012). Thus, studies in mice suggest that OX40 may play an important role in controlling immunity to pathogens that persist. This may also be the case in humans, as both HHV-8 and *Leishmania* establish persistent infections. However, the patient seemed to be able to control other persistent pathogens, including other herpes viruses, such as EBV and CMV, given their low viral loads in the blood (1,724 copies/ml and 102 IU/ml, respectively). The apparent integrity of central memory $CD4^+$ T cells, antigen-specific memory $CD8^+$ T cells, and antibody response may have been sufficient for protective immunity against these pathogens. The patient's specific susceptibility to HHV-8 and *Leishmania* may be a combinatorial consequence of the systemic deficit of effector memory $CD4^+$ T cells and the absence of OX40–OX40L-mediated

Downloaded from on November 4, 2016

Published July 29, 2013

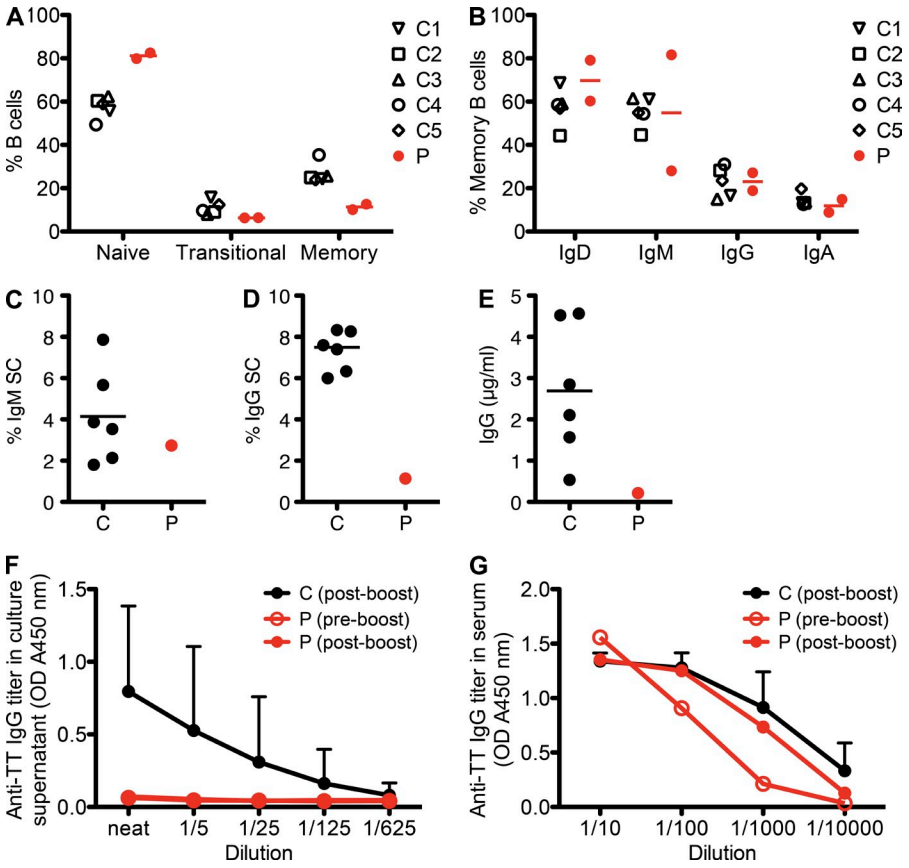


Figure 7. Low frequency of memory B cells but intact antibody response in vivo. (A) The proportions of B cell ($CD20^+$) subsets in PBMCs are shown. The various subsets were defined as follows: naive ($CD10^-CD27^-$), transitional ($CD10^+CD27^-$), and memory ($CD10^-CD27^+$). (B) The proportions of memory B cells from the patient and healthy controls expressing the indicated surface markers are shown. (C–F) Purified B cells from six age-matched healthy controls (C) and the patient (P) were cultured in the presence of CD40L, IL-10, IL-21, and CpG for 5 d. The frequencies of total IgM (C)- or IgG-secreting B cells (D) were assessed by ELISPOT. The levels of total IgG (E) or TT-specific secreted IgG (F) in the culture supernatant were quantified by ELISA. (A–E) Horizontal bars indicate the mean. (G) Anti-TT IgG titer in serum was assessed by ELISA. (F and G) Error bars indicate the SD from 6 (F) or 10 (G) healthy controls.

signaling at the disease site between T cells and endothelial/macrophage cells. Susceptibility to severe EBV infection in patients with X-linked lymphoproliferative disease is a classic example of a narrow infectious phenotype caused by the requirement for a specific co-stimulatory receptor–ligand interaction between T cells and EBV-infected antigen-presenting B cells (Hislop et al., 2010; Palendira et al., 2011, 2012). The full spectrum of infectious agents against which OX40-dependent immunity is critical will only become clear with the follow up of this patient and the identification of additional OX40-deficient individuals.

Finally, our study has important implications for clinical immunology, beyond the field of infectious diseases, in areas such as autoimmunity and tumor immunology. OX40 agonists have been shown to be effective for reducing cancer burden (Weinberg et al., 2011). Our study suggests that treatment with OX40 agonists might be particularly helpful in patients with KS. Conversely, blocking OX40–OX40L interaction has been considered a promising approach to the treatment of various diseases in which T cells play a critical role. In animal models, OX40L blockade in vivo has been shown to attenuate harmful diseases in many inflammatory and autoimmune models, including models of asthma, graft versus host disease, multiple sclerosis, rheumatoid arthritis, inflammatory bowel disease, and transplantation (Croft, 2010). Based on these findings, several clinical trials involving biological molecules targeting OX40 or OX40L are currently being considered or are already under way (http://clinicaltrials.gov). However, our findings suggest that a prolonged blockade of the interaction of OX40 with OX40L may lead to a predisposition to KS and perhaps VL. Close monitoring may therefore be warranted in future trials to decrease the likelihood or severity of such adverse events.

MATERIALS AND METHODS

Ethics statement. This study was conducted in accordance with the Helsinki Declaration, with written informed consent obtained from the patient and her family. Approval for this study was obtained from the Rockefeller University Institutional Review Board (New York), the Comité de Protection des Personnes (CPP) and Institut National de la Santé et de la Recherche

Downloaded from on November 4, 2016

Published July 29, 2013

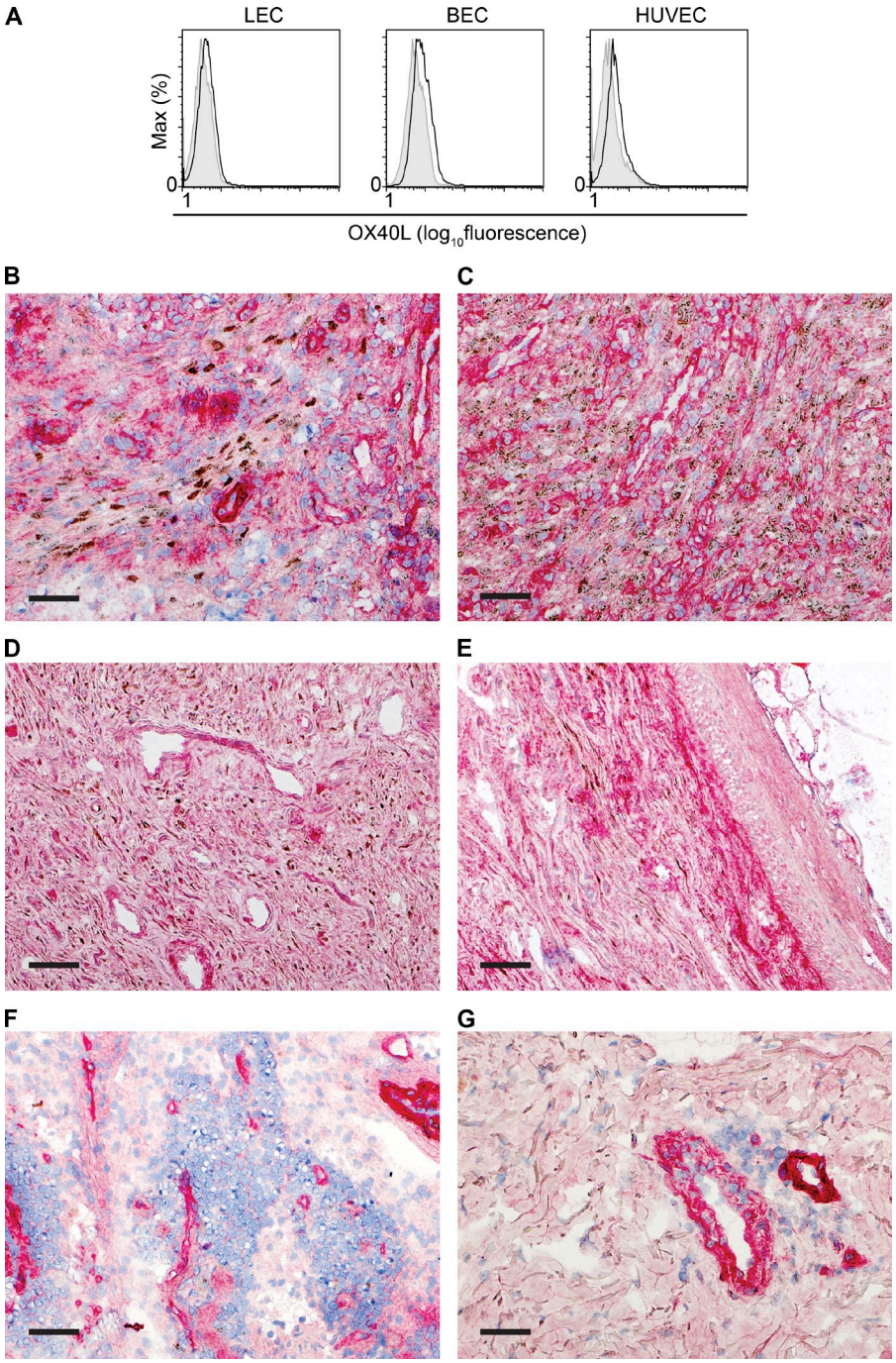


Figure 8. OX40L is abundantly expressed in KS lesions. (A) Expression of OX40L on the cell surface was assessed with flow cytometry in three types of primary endothelial cells: human dermal microvascular lymphatic endothelial cells (LEC), human dermal microvascular blood endothelial cells (BEC), and HUVECs. One result representative of two independent experiments is shown. (B–G) OX40L (red) and HHV-8 LANA (brown) expression was assessed by immunohistochemistry in frozen tissue sections. Bars, 5 mm. (B–E) AIDS-related KS lesions in lymph node (B), presenting as a submental mass (C), and in skin (D and E) show HHV-8–positive cells (punctate nuclear brown staining) as well as numerous OX40L-positive cells. (F and G) Non-KS tissues used as controls include normal lymph node (F) and skin with mycosis fungoides (G), showing OX40L in cells lining vascular spaces.

Médicale (France), and the human research ethics committees of the St.Vincent's Hospital and Sydney South West Area Health Service (Australia).

Case report. The detailed clinical case report for this patient has been published elsewhere (case 3 in Sahin et al. [2010]). Since the initial KS diagnosis, she has been sequentially treated with IFN-α, vinblastine, etoposide, and pegylated liposomal doxorubicin hydrochloride, with a partial response. The visceral lesions of KS regressed upon treatment, but widespread dermal lesions on the arms and legs remained. Blood samples were taken for leukocyte phenotyping and functional studies at least 6 mo after the last treatment.

Downloaded from on November 4, 2016

Published July 29, 2013

HHV-8 viremia, assessed by quantitative real-time PCR using primers specific to HHV-8 vCyclin, was negative in genomic DNA extracted from the patient's PBMCs.

Genotyping and linkage analysis. The patient and her parents were genotyped with the Affymetrix Genome-wide SNP 6.0 array, and the two unaffected siblings were genotyped with Affymetrix GeneChip Human Mapping 250K array. Genotype calling was achieved with Affymetrix Power Tools. We discarded monomorphic single nucleotide polymorphisms (SNPs), SNPs with a call rate <100%, and SNPs presenting more than one Mendelian inconsistency within the family. SNPs were further filtered with population-based filters. We then used 108,355 high-quality SNP markers to carry out linkage analysis, assuming autosomal recessive inheritance with complete penetrance (homozygosity mapping). Parametric multipoint linkage analysis was carried out with Merlin software (Abecasis et al., 2002). The Turkish family founders and HapMap CEU trios were used to estimate allele frequencies and to define linkage clusters, with an r^2 threshold of 0.4.

Whole-exome sequencing. Exome capture was performed with the SureSelect Human All Exon 50 Mb kit (Agilent Technologies). Paired-end sequencing was performed on a HiSeq 2000 (Illumina) generating 100-base reads. We aligned the sequences with the GRCh37 reference build of the human genome using the BWA aligner (Li and Durbin, 2009). Downstream processing and variant calling were performed with the Genome Analysis Toolkit (GATK; McKenna et al., 2010), SAMtools (Li et al., 2009), and Picard. Substitution and InDel calls were made with GATK Unified Genotyper. All calls with a read coverage ≤2x and a Phred-scaled SNP quality of ≤20 were filtered out. All variants were annotated using an annotation software system that was developed in-house.

Cell lines and retroviral and lentiviral transduction. Jurkat cells (ATCC) were grown in RPMI 1640 supplemented with 10% FBS. HEK-293 and Vero cells (ATCC) were grown in Dulbecco's Modified Eagle's Medium supplemented with 10% FBS. The human *TNFRSF4* cDNA (OriGene) was inserted into pMSCV-IRES-GFP (pMIG-OX40-WT). Site-directed mutagenesis was performed with the following primer pairs (bold indicates the base pairs in which mutations were introduced): 5′-GAACACGGTGTGC**T**GTCCGTGCGGG-3′ and 5′-CCCGCACGGAC**A**GCACACCGTGTTC-3′ for pMIG-OX40-R65C and 5′-GAACACGGTGTGC**GC**TCCGTGCGGGC-3′ and 5′-GCCCGCACGGA**GC**GCACACCGTGTTC-3′ for pMIG-OX40-R65A. Replication-incompetent retroviruses were produced with the GP2-293 packaging cell line (Takara Bio Inc.). Jurkat and HEK-293 cells were transduced with retroviruses in the presence of 3 μg/ml Polybrene (InvivoGen). Successfully transduced cells were identified as having a GFP signal (30–90% of live cells were GFP positive at the time of analysis). OX40-expressing lentiviral constructs were generated as previously described (Schoggins et al., 2011) with Gateway cloning technology (Life Technologies). In brief, OX40-WT and -R65C coding sequences were amplified by PCR from pMIG-OX40-WT and -R65C, respectively, with oligonucleotides containing *attB* sites flanking the coding sequence. The destination vector pTRIP.CMV.IVSb.iresTagRFP_Dest was provided by C. Rice (The Rockefeller University, New York, NY). Replication-incompetent lentiviruses were produced in HEK-293T cells and concentrated with Lenti-X concentrator (Takara Bio Inc.). PBMCs were activated by incubation with 5 μg/ml PHA for 24 h before the addition of lentiviruses. After 72 h of incubation with lentiviruses, cells were analyzed by flow cytometry. Successfully transduced cells were identified as positive for RFP (10–30% of live cells were RFP positive at the time of analysis).

Western blotting. Whole-cell lysates were prepared by incubating cell pellets with NP-40 lysis buffer (10 mM Tris HCl, pH 7.5, 150 mM NaCl, and 1% IGEPAL CA-630 [Sigma-Aldrich]) for 30 min on ice and then centrifuging at 20,000 *g*. OX40 immunoblotting was performed with a rabbit monoclonal antibody, EPR17Y (Epitomics). Antibodies against GAPDH (Santa Cruz Biotechnology, Inc.) and actin (Abgent) were used as for loading controls. When indicated, cell lysates were treated with endoglycosidase H or a combination of O-glycosidase and neuraminidase (New England Biolabs, Inc.) according to the manufacturer's instructions. Cell surface biotinylation was performed with the Pierce Cell Surface Protein Isolation kit (Thermo Fisher Scientific) according to the manufacturer's instructions.

Monitoring the UPR activation. PHA-activated T cell blasts were generated from PBMCs. T cell blasts were treated with DMSO alone, 1 μg/ml Brefeldin A (GolgiPlug; BD), or 1 μg/ml tunicamycin (Sigma-Aldrich) for 6 h. mRNA was extracted from the cells with an RNeasy Mini kit (QIAGEN), from which we synthesized cDNA with SuperScript III Reverse transcription (Life Technologies). For quantitative RT-PCR of BiP and GAPDH, we used TaqMan gene expression assays for human *HSPA5* (Hs00607129_gH; Applied Biosystems) and human *GAPDH* endogenous control (4310884E; Applied Biosystems). The following primer pair was used to detect the spliced variant of XBP1 by PCR: 5′-TTACGAGAGAAAACTCATGGCC-3′ and 5′-GGGTCCAAGTTGTCCAGAATGC-3′. The PCR products were separated and visualized in a 4% agarose gel.

Flow cytometry. Fluorochrome-conjugated antibodies against human CD3, CD4, CD8, CD10, CD20, CD25, CD27, CXCR5, CXCR3, IgD, IgM, IgG, IgA (BD), ACT35 clone directed against OX40, CD45RA (eBioscience), CCR7 (R&D Systems), CCR6, CD56, CD127, Vγδ (BioLegend), Vα24, and Vβ11 (Beckman Coulter) and the Live/Dead kit (Life Technologies) were used according to the manufacturers' instructions. Other antibodies against OX40, H-133 (Santa Cruz Biotechnology, Inc.), and EPR17Y (Epitomics) were used with Alexa Fluor 568–conjugated anti–rabbit Ig (Molecular Probes). Biotinylated recombinant human OX40L (Ancell) binding was detected with allophycocyanin-conjugated streptavidin (eBioscience). Virus-specific CD8 T cells were identified by staining PBMCs with specific soluble peptide–MHC multimers. CMV-specific cells were identified with HLA-A*0201–restricted pentamers (ProImmune) loaded with the NLVPMVATV peptide derived from pp65 (UL83) protein, and EBV-specific cells were identified with HLA-A*0201–restricted dextramers (Immudex) loaded with the GLCTLVAML peptide, derived from the lytic antigen BMLF-1. All data were collected on an LSRII flow cytometer (BD) and analyzed with FlowJo software (Tree Star).

Recall antigen assay. PBMCs were labeled with 1 μM CFSE at room temperature, in PBS supplemented with 5% FBS. CFSE-labeled PBMCs were incubated with various recall antigens for 5–6 d in RPMI 1640 supplemented with 10% FBS. The final concentrations and the source of recall antigens were as follows: 5 μg/ml tuberculin PPD, 7 Lf/ml TT (Statens Serum Institut), uninfected normal human dermal fibroblast (NHDF) extract, CMV-infected NHDF extract, VZV-infected NHDF extract, uninfected Vero cell extract, HSV-1–infected Vero cell extract, and 2.5–5 μg/ml EBV-infected human B cell extract (EastCoast Bio). PHA (Sigma-Aldrich) was used at a concentration of 5 μg/ml as a positive control. ELISA for cytokines was performed according to the manufacturer's protocol for IFN-γ (R&D Systems) and IL-10 (PeliPair).

In vitro B cell differentiation. Total B cells were purified from the OX40 patient as well as from six healthy controls using the Dynal negative selection kit (Invitrogen). B cells were cultured for 5 d with CD40L, 100 U/ml IL-10 (gift from DNAX), 50 ng/ml IL-21 (PeproTech), and 1 μg/ml CpG (Sigma-Aldrich). The frequency of IgM- and IgG-secreting cells was then determined by ELISPOT. Levels of total and TT-specific IgG in the 5-d culture were determined by ELISA (Avery et al., 2010).

Primary endothelial cells. Lymphatic endothelial cells (Lonza CC-2810), blood endothelial cells (Lonza CC-2811), and HUVECs (Lonza C2517A) were purchased from Lonza and cultured and maintained according to the manufacturer's instruction. The levels of TNF superfamily members on the cell surface were measured by flow cytometry. All data were collected on an LSRII flow cytometer and analyzed with FlowJo software.

Downloaded from on November 4, 2016

Published July 29, 2013

Immunohistochemistry. Double immunohistochemical staining of OX40L/LANA was accomplished by staining the two antibodies sequentially, using a Bond III Autostainer (Leica). For the first antibody OX40L (clone MM0505-8S23, 1:300; Novus Biologicals), after routine preparation (air-drying at room temperature for 1 h, then fixing in acetone for 10 min), frozen sections were subjected to sequential incubation with the dual endogenous enzyme block (Dako) for 5 min, primary antibody at 4°C for 16 h, post primary AP for 20 min, polymer AP for 30 min, and mixed red refine for 15 min (Bond Polymer Refine Red Detection; Leica). For the second antibody LANA (clone LN53, 1:500; Advanced Biotechnologies), OX40L-stained sections were incubated with the endogenous peroxidase block, primary antibody, post primary, polymer, diaminobenzidine, and hematoxylin for 5, 15, 8, 8, 10, and 5 min, respectively (Bond Polymer Refine Detection; Leica). Finally, sections were dehydrated in 100% ethanol and mounted in Cytoseal XYL (Thermo Fisher Scientific).

Estimation of the frequency of individuals with biallelic loss-of-function *TNFRSF4* mutations. We assumed that essential splice site mutations, frameshift mutations, stop-gain/loss mutations, and missense mutations that are predicted to be damaging by both PolyPhen-2 and SIFT may be deleterious (loss of function). Only two OX40 variants reported in the public databases (1000 Genomes and Exome Variant Server) fall under these categories: C31R (minor allele frequency 2.3×10^{-4}) and T62M (minor allele frequency 7.7×10^{-5}). Thus, the estimated frequency of individuals heterozygous for one of the possible loss-of-function OX40 alleles would be 6.2×10^{-4} ($= 2 \times [2.3 \times 10^{-4} + 7.7 \times 10^{-5}] \times [1 - 2.3 \times 10^{-4} - 7.7 \times 10^{-5}]$), and the frequency of biallelic carriers would be 9.5×10^{-8} ($= [2.3 \times 10^{-4} + 7.7 \times 10^{-5}]^2$).

Statistics. Prism software (GraphPad Software) was used to perform unpaired, one-tailed Student's *t* tests. Values of $P < 0.05$ were considered significant.

Online supplemental material. Table S1 shows genomic regions with positive LOD scores identified by homozygosity mapping of the patient and her family members. Table S2 lists variants unique to the patient that are homozygous and within the intervals identified by linkage analysis. Online supplemental material is available at http://www.jem.org/cgi/content/full/jem.20130592/DC1.

We thank the patient and her family for participating in our study, all members of the laboratory, Saida Dadi, and Mary Ellen Conley for their discussions, and Charles Rice for kindly providing destination vectors.

The Laboratory of Human Genetics of Infectious Diseases is supported by grants from the Institut National de la Santé et de la Recherche Médicale, University Paris Descartes, the French Government's Investissement d'Avenir program, Laboratoire d'Excellence "Integrative Biology of Emerging Infectious Diseases" (ANR-10-LABX-62-IBEID), the St. Giles Foundation, the National Center for Research Resources and the National Center for Advancing Sciences (NCATS) grant number 8UL1TR000043 from the National Institutes of Health, and the Rockefeller University. M. Byun is supported by the Charles H. Revson Foundation and formerly by the Irvington Institute Fellowship Program of the Cancer Research Institute. C.S. Ma, U. Palendira, and S.G. Tangye are supported by the National Health and Medical Research Council of Australia and Cancer Council New South Wales. E. Cesarman is funded by National Institutes of Health grants R01CA103646 and R01CA154228.

J.-L. Casanova is a member of the Sanofi Strategic Development and Scientific Advisory Committee. The authors have no additional conflicting financial interests.

Submitted: 21 March 2013
Accepted: 9 July 2013

REFERENCES

Abecasis, G.R., S.S. Cherny, W.O. Cookson, and L.R. Cardon. 2002. Merlin—rapid analysis of dense genetic maps using sparse gene flow trees. *Nat. Genet.* 30:97–101. http://dx.doi.org/10.1038/ng786

Adzhubei, I.A., S. Schmidt, L. Peshkin, V.E. Ramensky, A. Gerasimova, P. Bork, A.S. Kondrashov, and S.R. Sunyaev. 2010. A method and server for predicting damaging missense mutations. *Nat. Methods.* 7:248–249. http://dx.doi.org/10.1038/nmeth0410-248

Akman, E.S., U. Ertem, V. Tankal, A. Pamir, A.M. Tuncer, and O. Uluoğlu. 1989. Aggressive Kaposi's sarcoma in children: a case report. *Turk. J. Pediatr.* 31:297–303.

Alcaïs, A., L. Quintana-Murci, D.S. Thaler, E. Schurr, L. Abel, and J.L. Casanova. 2010. Life-threatening infectious diseases of childhood: single-gene inborn errors of immunity? *Ann. N.Y. Acad. Sci.* 1214:18–33. http://dx.doi.org/10.1111/j.1749-6632.2010.05834.x

Andreoni, M., G. El-Sawaf, G. Rezza, B. Ensoli, E. Nicastri, L. Ventura, L. Ercoli, L. Sarmati, and G. Rocchi. 1999. High seroprevalence of antibodies to human herpesvirus-8 in Egyptian children: evidence of non-sexual transmission. *J. Natl. Cancer Inst.* 91:465–469. http://dx.doi.org/10.1093/jnci/91.5.465

Andreoni, M., L. Sarmati, E. Nicastri, G. El Sawaf, M. El Zalabani, I. Uccella, R. Bugarini, S.G. Parisi, and G. Rezza. 2002. Primary human herpesvirus 8 infection in immunocompetent children. *JAMA.* 287:1295–1300. http://dx.doi.org/10.1001/jama.287.10.1295

Avery, D.T., E.K. Deenick, C.S. Ma, S. Suryani, N. Simpson, G.Y. Chew, T.D. Chan, U. Palendira, J. Bustamante, S. Boisson-Dupuis, et al. 2010. B cell–intrinsic signaling through IL-21 receptor and STAT3 is required for establishing long-lived antibody responses in humans. *J. Exp. Med.* 207:155–171. http://dx.doi.org/10.1084/jem.20091706

Bisceglia, M., M. Amini, and C. Bosman. 1988. Primary Kaposi's sarcoma of the lymph node in children. *Cancer.* 61:1715–1718. http://dx.doi.org/10.1002/1097-0142(19880415)61:8<1715::AID-CNCR2820610833>3.0.CO;2-P

Boettler, T., F. Moeckel, Y. Cheng, M. Heeg, S. Salek-Ardakani, S. Crotty, M. Croft, and M.G. von Herrath. 2012. OX40 facilitates control of a persistent virus infection. *PLoS Pathog.* 8:e1002913. http://dx.doi.org/10.1371/journal.ppat.1002913

Boshoff, C., and R.A. Weiss. 2001. Epidemiology and pathogenesis of Kaposi's sarcoma-associated herpesvirus. *Philos. Trans. R. Soc. Lond. B Biol. Sci.* 356:517–534. http://dx.doi.org/10.1098/rstb.2000.0778

Bryant, V.L., C.S. Ma, D.T. Avery, Y. Li, K.L. Good, L.M. Corcoran, R. de Waal Malefyt, and S.G. Tangye. 2007. Cytokine-mediated regulation of human B cell differentiation into Ig-secreting cells: predominant role of IL-21 produced by CXCR5+ T follicular helper cells. *J. Immunol.* 179:8180–8190.

Bucheton, B., L. Abel, S. El-Safi, M.M. Kheir, S. Pavek, A. Lemainque, and A.J. Dessein. 2003. A major susceptibility locus on chromosome 22q12 plays a critical role in the control of kala-azar. *Am. J. Hum. Genet.* 73:1052–1060. http://dx.doi.org/10.1086/379084

Byun, M., A. Abhyankar, V. Lelarge, S. Plancoulaine, A. Palanduz, L. Telhan, B. Boisson, C. Picard, S. Dewell, C. Zhao, et al. 2010. Whole-exome sequencing-based discovery of STIM1 deficiency in a child with fatal classic Kaposi sarcoma. *J. Exp. Med.* 207:2307–2312. http://dx.doi.org/10.1084/jem.20101597

Cabello, P.H., A.M. Lima, E.S. Azevedo, and H. Krieger. 1995. Familial aggregation of *Leishmania chagasi* infection in northeastern Brazil. *Am. J. Trop. Med. Hyg.* 52:364–365.

Cakir, F.B., E. Cakir, N. Tuzuner, and A. Kut. 2013. Classic Kaposi sarcoma with pulmonary involvement mimicking endobronchial tuberculosis in a child. *Pediatr. Pulmonol.* 48:310–312. http://dx.doi.org/10.1002/ppul.22635

Camcioglu, Y., C. Picard, V. Lacoste, S. Dupuis, N. Akçakaya, H. Cokura, G. Kaner, C. Demirkesen, S. Plancoulaine, J.F. Emile, et al. 2004. HHV-8-associated Kaposi sarcoma in a child with IFNgammaR1 deficiency. *J. Pediatr.* 144:519–523. http://dx.doi.org/10.1016/j.jpeds.2003.11.012

Cann, H.M., C. de Toma, L. Cazes, M.F. Legrand, V. Morel, L. Piouffre, J. Bodmer, W.F. Bodmer, B. Bonne-Tamir, A. Cambon-Thomsen, et al. 2002. A human genome diversity cell line panel. *Science.* 296:261–262. http://dx.doi.org/10.1126/science.296.5566.261b

Casanova, J.L., and L. Abel. 2007. Primary immunodeficiencies: a field in its infancy. *Science.* 317:617–619. http://dx.doi.org/10.1126/science.1142963

Chang, Y., E. Cesarman, M.S. Pessin, F. Lee, J. Culpepper, D.M. Knowles, and P.S. Moore. 1994. Identification of herpesvirus-like DNA sequences in AIDS-associated Kaposi's sarcoma. *Science.* 266:1865–1869. http://dx.doi.org/10.1126/science.7997879

Downloaded from on November 4, 2016

Published July 29, 2013

Chappuis, F., S. Sundar, A. Hailu, H. Ghalib, S. Rijal, R.W. Peeling, J. Alvar, and M. Boelaert. 2007. Visceral leishmaniasis: what are the needs for diagnosis, treatment and control? *Nat. Rev. Microbiol.* 5:873–882. http://dx.doi.org/10.1038/nrmicro1748

Compaan, D.M., and S.G. Hymowitz. 2006. The crystal structure of the costimulatory OX40-OX40L complex. *Structure.* 14:1321–1330. http://dx.doi.org/10.1016/j.str.2006.06.015

Conley, M.E., A.K. Dobbs, D.M. Farmer, S. Kilic, K. Paris, S. Grigoriadou, E. Coustan-Smith, V. Howard, and D. Campana. 2009. Primary B cell immunodeficiencies: comparisons and contrasts. *Annu. Rev. Immunol.* 27:199–227. http://dx.doi.org/10.1146/annurev.immunol.021908.132649

Croft, M. 2003. Co-stimulatory members of the TNFR family: keys to effective T-cell immunity? *Nat. Rev. Immunol.* 3:609–620. http://dx.doi.org/10.1038/nri1148

Croft, M. 2010. Control of immunity by the TNFR-related molecule OX40 (CD134). *Annu. Rev. Immunol.* 28:57–78. http://dx.doi.org/10.1146/annurev-immunol-030409-101243

Davidovici, B., I. Karakis, D. Bourboulia, S. Ariad, J. Zong, D. Benharroch, N. Dupin, R. Weiss, G. Hayward, B. Sarov, and C. Boshoff. 2001. Seroepidemiology and molecular epidemiology of Kaposi's sarcoma-associated herpesvirus among Jewish population groups in Israel. *J. Natl. Cancer Inst.* 93:194–202. http://dx.doi.org/10.1093/jnci/93.3.194

de Beaucoudrey, L., A. Samarina, J. Bustamante, A. Cobat, S. Boisson-Dupuis, J. Feinberg, S. Al-Muhsen, L. Jannière, Y. Rose, M. de Suremain, et al. 2010. Revisiting human IL-12Rβ1 deficiency: a survey of 141 patients from 30 countries. *Medicine (Baltimore).* 89:381–402. http://dx.doi.org/10.1097/MD.0b013e3181fdd832

Duhen, T., R. Duhen, A. Lanzavecchia, F. Sallusto, and D.J. Campbell. 2012. Functionally distinct subsets of human FOXP3+ Treg cells that phenotypically mirror effector Th cells. *Blood.* 119:4430–4440. http://dx.doi.org/10.1182/blood-2011-11-392324

Dutz, W., and A.P. Stout. 1960. Kaposi's sarcoma in infants and children. *Cancer.* 13:684–694. http://dx.doi.org/10.1002/1097-0142(196007/08)13:4<684::AID-CNCR2820130408>3.0.CO;2-G

Ferrari, A., M. Casanova, G. Bisogno, G. Cecchetto, C. Meazza, L. Gandola, A. Garaventa, A. Mattke, J. Treuner, and M. Carli. 2002. Malignant vascular tumors in children and adolescents: a report from the Italian and German Soft Tissue Sarcoma Cooperative Group. *Med. Pediatr. Oncol.* 39:109–114. http://dx.doi.org/10.1002/mpo.10078

Fuchs, S., A. Rensing-Ehl, C. Speckmann, B. Bengsch, A. Schmitt-Graeff, I. Bondzio, A. Maul-Pavicic, T. Bass, T. Vraetz, B. Strahm, et al. 2012. Antiviral and regulatory T cell immunity in a patient with stromal interaction molecule 1 deficiency. *J. Immunol.* 188:1523–1533. http://dx.doi.org/10.4049/jimmunol.1102507

Ganem, D. 2010. KSHV and the pathogenesis of Kaposi sarcoma: listening to human biology and medicine. *J. Clin. Invest.* 120:939–949. http://dx.doi.org/10.1172/JCI40567

Gessain, A., P. Mauclère, M. van Beveren, S. Plancoulaine, A. Ayouba, J.L. Essame-Oyono, P.M. Martin, and G. de Thé. 1999. Human herpesvirus 8 primary infection occurs during childhood in Cameroon, Central Africa. *Int. J. Cancer.* 81:189–192. http://dx.doi.org/10.1002/(SICI)1097-0215(19990412)81:2<189::AID-IJC4>3.0.CO;2-E

Gramaglia, I., A. Jember, S.D. Pippig, A.D. Weinberg, N. Killeen, and M. Croft. 2000. The OX40 costimulatory receptor determines the development of CD4 memory by regulating primary clonal expansion. *J. Immunol.* 165:3043–3050.

Hendriks, J., Y. Xiao, J.W. Rossen, K.F. van der Sluijs, K. Sugamura, N. Ishii, and J. Borst. 2005. During viral infection of the respiratory tract, CD27, 4-1BB, and OX40 collectively determine formation of CD8+ memory T cells and their capacity for secondary expansion. *J. Immunol.* 175:1665–1676.

Hislop, A.D., U. Palendira, A.M. Leese, P.D. Arkwright, P.S. Rohrlich, S.G. Tangye, H.B. Gaspar, A.C. Lankester, A. Moretta, and A.B. Rickinson. 2010. Impaired Epstein-Barr virus-specific CD8+ T-cell function in X-linked lymphoproliferative disease is restricted to SLAM family-positive B-cell targets. *Blood.* 116:3249–3257. http://dx.doi.org/10.1182/blood-2009-09-238832

Humphreys, I.R., A. Loewendorf, C. de Trez, K. Schneider, C.A. Benedict, M.W. Munks, C.F. Ware, and M. Croft. 2007. OX40 costimulation promotes persistence of cytomegalovirus-specific CD8 T Cells: A CD4-dependent mechanism. *J. Immunol.* 179:2195–2202.

Hussein, M.R. 2008. Cutaneous and lymphadenopathic Kaposi's sarcoma: a case report and review of literature. *J. Cutan. Pathol.* 35:575–578. http://dx.doi.org/10.1111/j.1600-0560.2007.00844.x

Ibrahim, M.E., B. Lambson, A.O. Yousif, N.S. Deifalla, D.A. Alnaiem, A. Ismail, H. Yousif, H.W. Ghalib, E.A. Khalil, A. Kadaro, et al. 1999. Kala-azar in a high transmission focus: an ethnic and geographic dimension. *Am. J. Trop. Med. Hyg.* 61:941–944.

Imura, A., T. Hori, K. Imada, T. Ishikawa, Y. Tanaka, M. Maeda, S. Imamura, and T. Uchiyama. 1996. The human OX40/gp34 system directly mediates adhesion of activated T cells to vascular endothelial cells. *J. Exp. Med.* 183:2185–2195. http://dx.doi.org/10.1084/jem.183.5.2185

Iscovich, J., P. Boffetta, S. Franceschi, E. Azizi, and R. Sarid. 2000. Classic Kaposi sarcoma: epidemiology and risk factors. *Cancer.* 88:500–517. http://dx.doi.org/10.1002/(SICI)1097-0142(20000201)88:3<500::AID-CNCR3>3.0.CO;2-9

Jensen, P., S. Hansen, B. Møller, T. Leivestad, P. Pfeffer, O. Geiran, P. Fauchald, and S. Simonsen. 1999. Skin cancer in kidney and heart transplant recipients and different long-term immunosuppressive therapy regimens. *J. Am. Acad. Dermatol.* 40:177–186. http://dx.doi.org/10.1016/S0190-9622(99)70185-4

Kaposi, M. 1872. Idiopathisches multiples pigmentsarcom der haut. *Arch Dermatol und Syphillis.* 4:265–273.

Khalil, E.A., E.E. Zijlstra, P.A. Kager, and A.M. El Hassan. 2002. Epidemiology and clinical manifestations of *Leishmania donovani* infection in two villages in an endemic area in eastern Sudan. *Trop. Med. Int. Health.* 7:35–44. http://dx.doi.org/10.1046/j.1365-3156.2002.00832.x

Kopf, M., C. Ruedl, N. Schmitz, A. Gallimore, K. Lefrang, B. Ecabert, B. Odermatt, and M.F. Bachmann. 1999. OX40-deficient mice are defective in Th cell proliferation but are competent in generating B cell and CTL Responses after virus infection. *Immunity.* 11:699–708. http://dx.doi.org/10.1016/S1074-7613(00)80144-2

Kumar, P., S. Henikoff, and P.C. Ng. 2009. Predicting the effects of coding non-synonymous variants on protein function using the SIFT algorithm. *Nat. Protoc.* 4:1073–1081. http://dx.doi.org/10.1038/nprot.2009.86

Kumar, R., and S. Nylén. 2012. Immunobiology of visceral leishmaniasis. *Front Immunol.* 3:251.

Kunitomi, A., T. Hori, A. Imura, and T. Uchiyama. 2000. Vascular endothelial cells provide T cells with costimulatory signals via the OX40/gp34 system. *J. Leukoc. Biol.* 68:111–118.

Landau, H.J., B.J. Poiesz, S. Dube, J.A. Bogart, L.B. Weiner, and A.K. Souid. 2001. Classic Kaposi's sarcoma associated with human herpesvirus 8 infection in a 13-year-old male: a case report. *Clin. Cancer Res.* 7:2263–2268.

Lebbé, C., C. Legendre, and C. Francès. 2008. Kaposi sarcoma in transplantation. *Transplant. Rev. (Orlando).* 22:252–261. http://dx.doi.org/10.1016/j.trre.2008.05.004

Li, H., and R. Durbin. 2009. Fast and accurate short read alignment with Burrows-Wheeler transform. *Bioinformatics.* 25:1754–1760. http://dx.doi.org/10.1093/bioinformatics/btp324

Li, H., B. Handsaker, A. Wysoker, T. Fennell, J. Ruan, N. Homer, G. Marth, G. Abecasis, and R. Durbin; 1000 Genome Project Data Processing Subgroup. 2009. The Sequence Alignment/Map format and SAMtools. *Bioinformatics.* 25:2078–2079. http://dx.doi.org/10.1093/bioinformatics/btp352

Mayama, S., L.E. Cuevas, J. Sheldon, O.H. Omar, D.H. Smith, P. Okong, B. Silvel, C.A. Hart, and T.F. Schulz. 1998. Prevalence and transmission of Kaposi's sarcoma-associated herpesvirus (human herpesvirus 8) in Ugandan children and adolescents. *Int. J. Cancer.* 77:817–820. http://dx.doi.org/10.1002/(SICI)1097-0215(19980911)77:6<817::AID-IJC2>3.0.CO;2-X

McKenna, A.H., M. Hanna, E. Banks, A. Sivachenko, K. Cibulskis, A. Kernytsky, K. Garimella, D. Altshuler, S. Gabriel, M. Daly, and M.A. DePristo. 2010. The Genome Analysis Toolkit: a MapReduce framework for analyzing next-generation DNA sequencing data. *Genome Res.* 20:1297–1303. http://dx.doi.org/10.1101/gr.107524.110

Michel, G., C. Pomares, B. Ferrua, and P. Marty. 2011. Importance of worldwide asymptomatic carriers of *Leishmania infantum* (*L. chagasi*) in human. *Acta Trop.* 119:69–75. http://dx.doi.org/10.1016/j.actatropica.2011.05.012

Downloaded from on November 4, 2016

Published July 29, 2013

Morimoto, S., Y. Kanno, Y. Tanaka, Y. Tokano, H. Hashimoto, S. Jacquot, C. Morimoto, S.F. Schlossman, H. Yagita, K. Okumura, and T. Kobata. 2000. CD134L engagement enhances human B cell Ig production: CD154/CD40, CD70/CD27, and CD134/CD134L interactions coordinately regulate T cell-dependent B cell responses. *J. Immunol.* 164: 4097–4104.

Murray, H.W. 1999. Kala-azar as an AIDS-related opportunistic infection. *AIDS Patient Care STDS.* 13:459–465. http://dx.doi.org/10.1089/108729199318183

Olweny, C.L., A. Kaddumukasa, I. Atine, R. Owor, I. Magrath, and J.L. Ziegler. 1976. Childhood Kaposi's sarcoma: clinical features and therapy. *Br. J. Cancer.* 33:555–560. http://dx.doi.org/10.1038/bjc.1976.88

Palendira, U., C. Low, A. Chan, A.D. Hislop, E. Ho, T.G. Phan, E. Deenick, M.C. Cook, D.S. Riminton, S. Choo, et al. 2011. Molecular pathogenesis of EBV susceptibility in XLP as revealed by analysis of female carriers with heterozygous expression of SAP. *PLoS Biol.* 9:e1001187. http://dx.doi.org/10.1371/journal.pbio.1001187

Palendira, U., C. Low, A.I. Bell, C.S. Ma, R.J. Abbott, T.G. Phan, D.S. Riminton, S. Choo, J.M. Smart, V. Lougaris, et al. 2012. Expansion of somatically reverted memory $CD8^+$ T cells in patients with X-linked lymphoproliferative disease caused by selective pressure from Epstein-Barr virus. *J. Exp. Med.* 209:913–924. http://dx.doi.org/10.1084/jem.20112391

Papadopoulos, C., G. Terzis, G.K. Papadimas, and P. Manta. 2013. OX40-OX40L expression in idiopathic inflammatory myopathies. *Anal. Quant. Cytol. Histol.* 35:17–26.

Picard, C., F. Mellouli, R. Duprez, G. Chédeville, B. Neven, S. Fraitag, J. Delaunay, F. Le Deist, A. Fischer, S. Blanche, et al. 2006. Kaposi's sarcoma in a child with Wiskott-Aldrich syndrome. *Eur. J. Pediatr.* 165:453–457. http://dx.doi.org/10.1007/s00431-006-0107-2

Pippig, S.D., C. Peña-Rossi, J. Long, W.R. Godfrey, D.J. Fowell, S.L. Reiner, M.L. Birkeland, R.M. Locksley, A.N. Barclay, and N. Killeen. 1999. Robust B cell immunity but impaired T cell proliferation in the absence of CD134 (OX40). *J. Immunol.* 163:6520–6529.

Plancoulaine, S., L. Abel, M. van Beveren, D.A. Trégouët, M. Joubert, P. Tortevoye, G. de Thé, and A. Gessain. 2000. Human herpesvirus 8 transmission from mother to child and between siblings in an endemic population. *Lancet*.356:1062–1065.http://dx.doi.org/10.1016/S0140-6736(00)02729-X

Plancoulaine, S., L. Abel, and A. Gessain. 2002. [Epidemiology of human herpes virus 8 (HHV-8) or the herpes virus associated with Kaposi's sarcoma (KSHV)]. *Pathol. Biol. (Paris).* 50:496–502. http://dx.doi.org/10.1016/S0369-8114(02)00317-6

Sahin, G., A. Palanduz, G. Aydogan, O. Cassar, A.U. Ertem, L. Telhan, N. Canpolat, E. Jouanguy, C. Picard, A. Gessain, et al. 2010. Classic Kaposi sarcoma in 3 unrelated Turkish children born to consanguineous kindreds. *Pediatrics.* 125:e704–e708. http://dx.doi.org/10.1542/peds.2009-2224

Salek-Ardakani, S., M. Moutaftsi, S. Crotty, A. Sette, and M. Croft. 2008. OX40 drives protective vaccinia virus-specific CD8 T cells. *J. Immunol.* 181:7969–7976.

Salem, H.A., M. El Sohafy, and M. Abd El Gawad. 2011. Kaposi's sarcoma in an atopic dermatitis patient: a case report and a review of literature. *Pediatr. Dermatol.* 28:547–549. http://dx.doi.org/10.1111/j.1525-1470.2011.01347.x

Sanal, O., G. Turkkani, F. Gumruk, L. Yel, G. Secmeer, I. Tezcan, A. Kara, and F. Ersoy. 2007. A case of interleukin-12 receptor beta-1 deficiency with recurrent leishmaniasis. *Pediatr. Infect. Dis. J.* 26:366–368. http://dx.doi.org/10.1097/01.inf.0000258696.64507.0f

Schoggins, J.W., S.J. Wilson, M. Panis, M.Y. Murphy, C.T. Jones, P. Bieniasz, and C.M. Rice. 2011. A diverse range of gene products are effectors of the type I interferon antiviral response. *Nature.* 472:481–485. http://dx.doi.org/10.1038/nature09907

Serraino, D., P. Piselli, C. Angeletti, E. Minetti, A. Pozzetto, G. Civati, S. Bellelli, F. Farchi, F. Citterio, G. Rezza, et al. 2005. Risk of Kaposi's sarcoma and of other cancers in Italian renal transplant patients. *Br. J. Cancer.* 92:572–575.

Shiels, M.S., R.M. Pfeiffer, M.H. Gail, H.I. Hall, J. Li, A.K. Chaturvedi, K. Bhatia, T.S. Uldrick, R. Yarchoan, J.J. Goedert, and E.A. Engels. 2011. Cancer burden in the HIV-infected population in the United States. *J. Natl. Cancer Inst.* 103:753–762. http://dx.doi.org/10.1093/jnci/djr076

Souza, H.S., C.C. Elia, J. Spencer, and T.T. MacDonald. 1999. Expression of lymphocyte-endothelial receptor-ligand pairs, alpha4beta7/MAdCAM-1 and OX40/OX40 ligand in the colon and jejunum of patients with inflammatory bowel disease. *Gut.* 45:856–863. http://dx.doi.org/10.1136/gut.45.6.856

Taylor, J.F., P.G. Smith, D. Bull, and M.C. Pike. 1972. Kaposi's sarcoma in Uganda: geographic and ethnic distribution. *Br. J. Cancer.* 26:483–497. http://dx.doi.org/10.1038/bjc.1972.66

Wang, Q.J., F.J. Jenkins, L.P. Jacobson, L.A. Kingsley, R.D. Day, Z.W. Zhang, Y.X. Meng, P.E. Pellett, K.G. Kousoulas, A. Baghian, and C.R. Rinaldo Jr. 2001. Primary human herpesvirus 8 infection generates a broadly specific CD8(+) T-cell response to viral lytic cycle proteins. *Blood.* 97:2366–2373. (published erratum appears in *Blood*. 2002. 99:3499) http://dx.doi.org/10.1182/blood.V97.8.2366

Weinberg, A.D., N.P. Morris, M. Kovacsovics-Bankowski, W.J. Urba, and B.D. Curti. 2011. Science gone translational: the OX40 agonist story. *Immunol. Rev.* 244:218–231. http://dx.doi.org/10.1111/j.1600-065X.2011.01069.x

Zubairi, S., S.L. Sanos, S. Hill, and P.M. Kaye. 2004. Immunotherapy with OX40L-Fc or anti-CTLA-4 enhances local tissue responses and killing of *Leishmania donovani*. *Eur. J. Immunol.* 34:1433–1440. http://dx.doi.org/10.1002/eji.200324021

Zurrida, S., R. Agresti, and G. Cefalo. 1994. Juvenile classic Kaposi's sarcoma: a report of two cases, one with family history. *Pediatr. Hematol. Oncol.* 11:409–416. http://dx.doi.org/10.3109/08880019409140540

Downloaded from on November 4, 2016